Coherent emission from relativistic magnetized shocks: a source of FRBs?

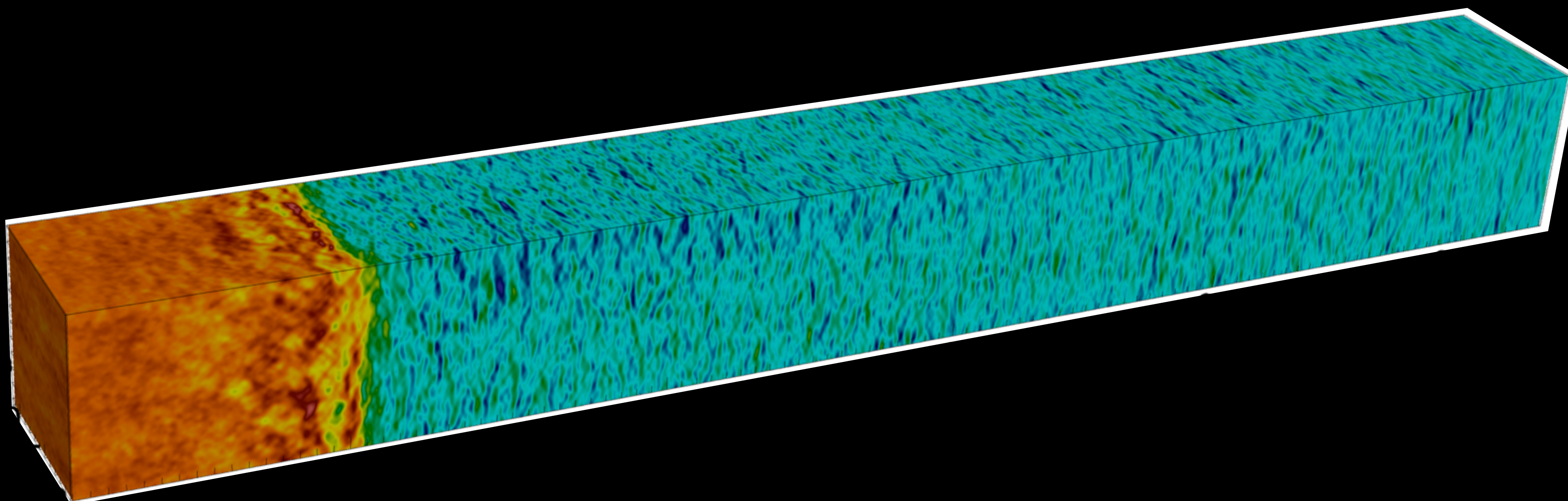

Lorenzo Sironi (Columbia)

with: A. Babul, J. Nattila, I. Plotnikov, E. Sobacchi, N. Sridhar, A. Beloborodov, Y. Lyubarsky, B. Margalit, B. Metzger

Coherent emission in FRBs

Why do FRBs require coherent emission?

$$T_{\rm B} = \frac{S_\nu D_{\rm A}^2}{2\pi t_{\rm FRB}^2 \nu^2 k_{\rm B}} \simeq (1.1\times 10^{35}\ {\rm K})\ \frac{S_\nu}{\rm Jy}\left(\frac{D_{\rm A}}{\rm Gpc}\right)^2 t_{{\rm FRB},-3}^{-2}\nu_9^{-2}$$

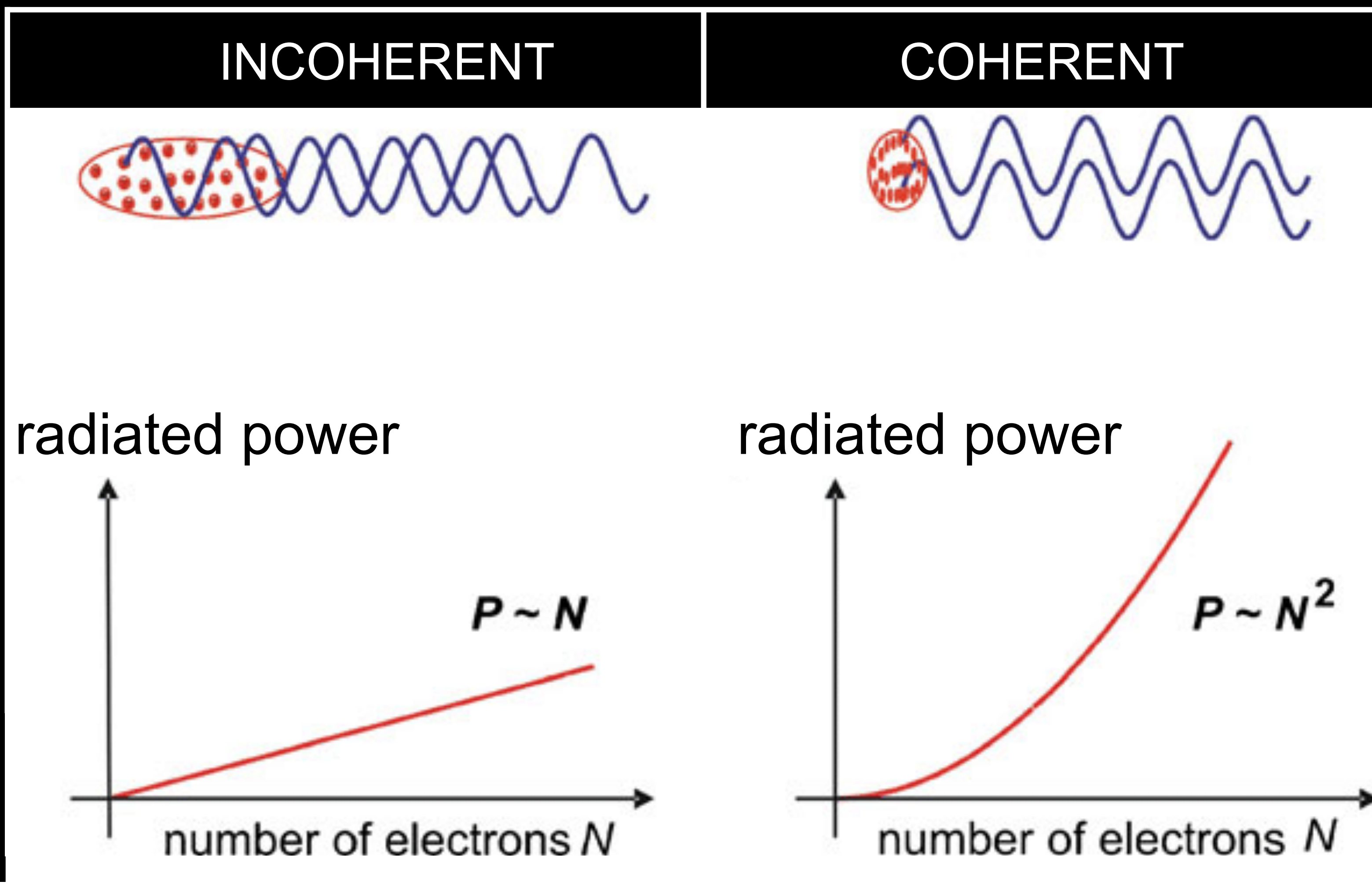

Coherent emission mechanisms

[Melrose 86]

• Antenna:

• Bunches of electrons localized in space and momentum, radiating as a macro-charge.

• Back reaction leads to spreading in space, and self-suppression.

• Reactive instability:

• Localization in momentum leads to self-bunching and phase-coherent wave growth.

• Back reaction leads to spreading in momentum, and self-suppression when the spread causes the bandwidth to exceed the growth rate.

• Maser instability:

• Population inversion, with growth corresponding to negative absorption.

• Back reaction leads to relaxation of the population inversion.

FRBs from magnetars

- Energy may be released by a “magnetar quake”, launching Alfven waves

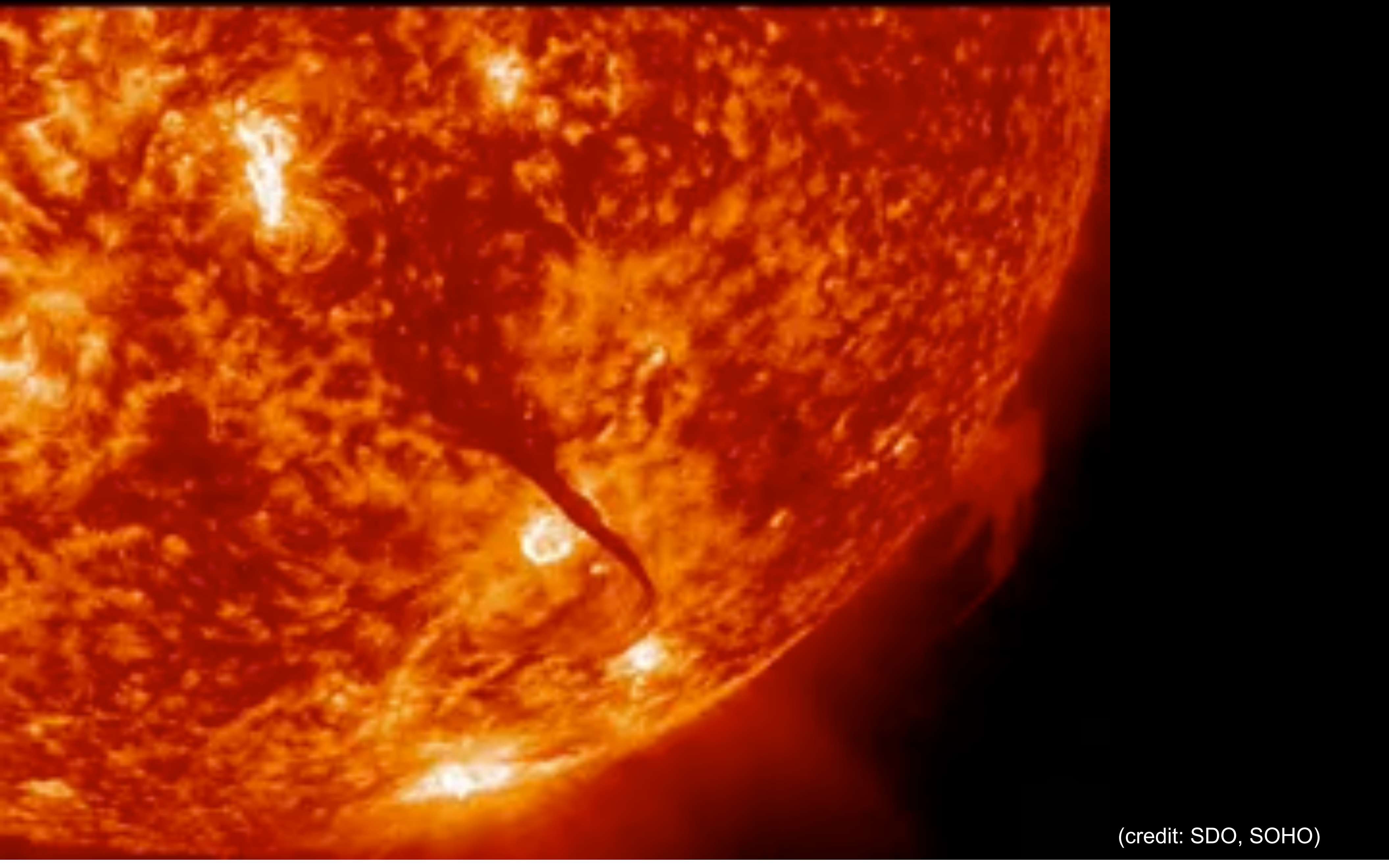

(credit: SDO, SOHO)

FRBs from magnetars

- Energy may be released by a "magnetar quake", launching Alfven waves
- Alfven waves become nonlinear, driving magnetic reconnection and shocks

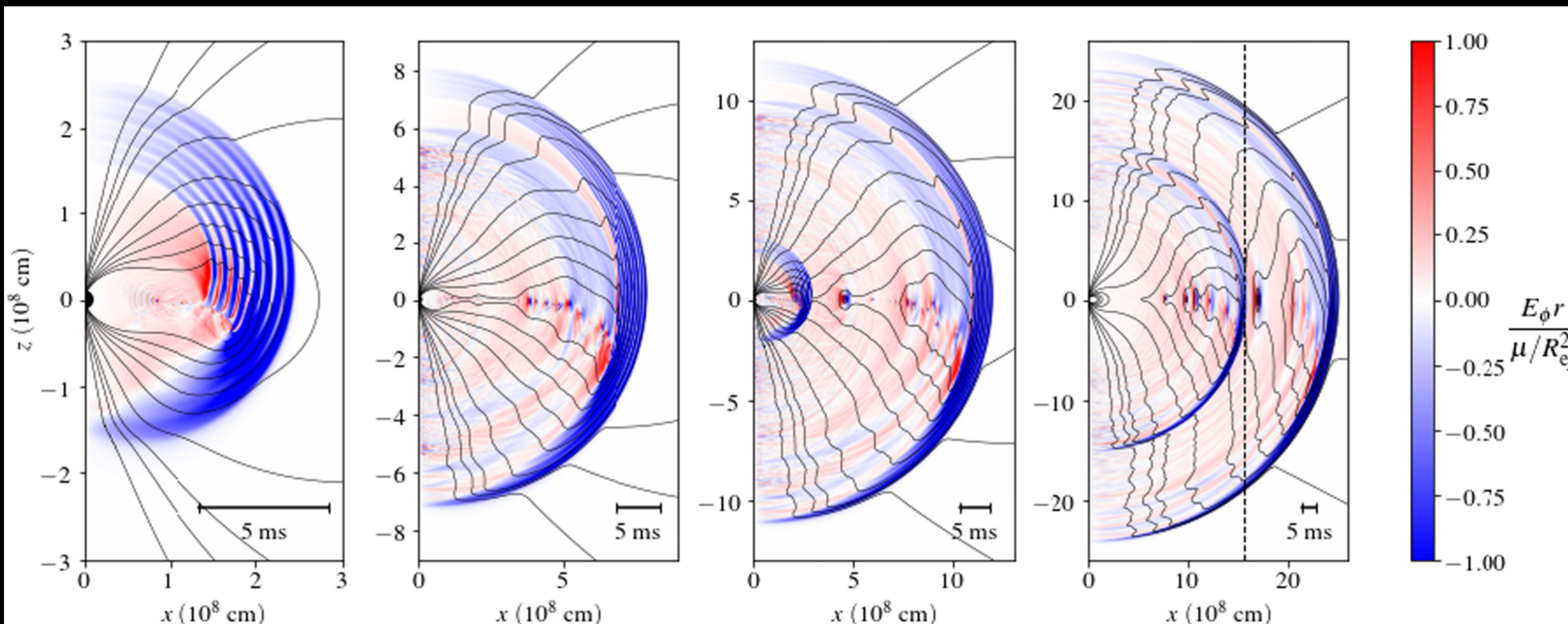

(Yuan+ 20)

- Sites of FRB generation:
  - inner magnetosphere via antenna (e.g., talks by Kumar, Lu, Zhang)
  - outer magnetosphere via reconnection (Lyubarsky 20)
  - blast wave / shock (Lyubarsky 14, Metzger+ 19, Beloborodov 20)

Coherent emission from reconnection

• Relativistic reconnection, with large "magnetization" $\sigma = \dfrac{B_0^2}{4\pi\rho c^2} \gg 1$

is highly dynamical, with copious formation of plasmoids.

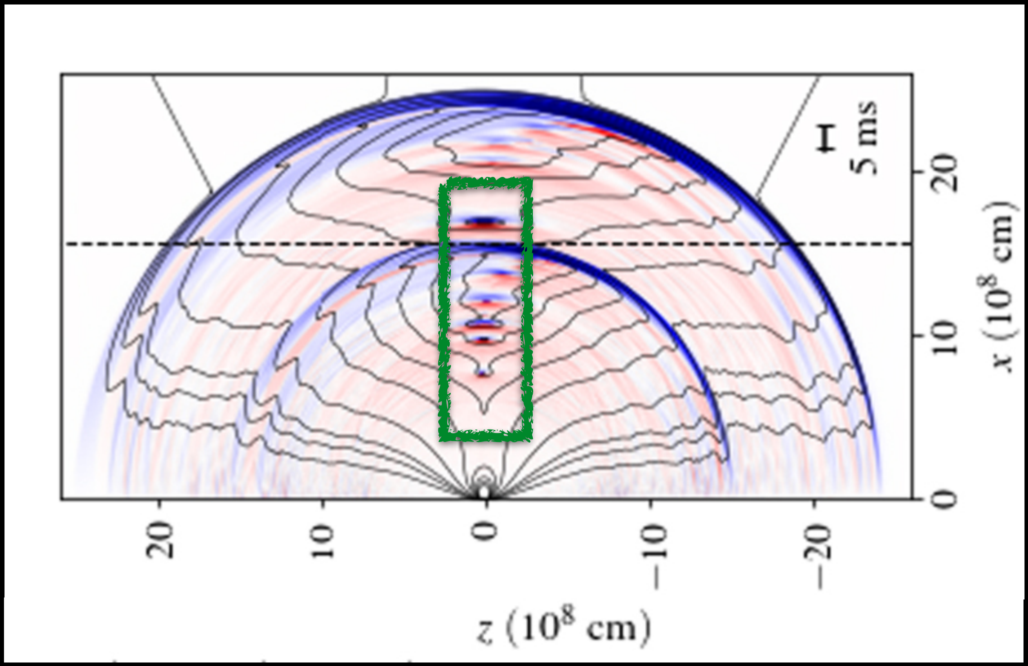

(Yuan+ 20)

Coherent emission from reconnection

- Relativistic reconnection, with large "magnetization" $\sigma = \dfrac{B_0^2}{4\pi \rho c^2} \gg 1$

is highly dynamical, with copious formation of plasmoids.

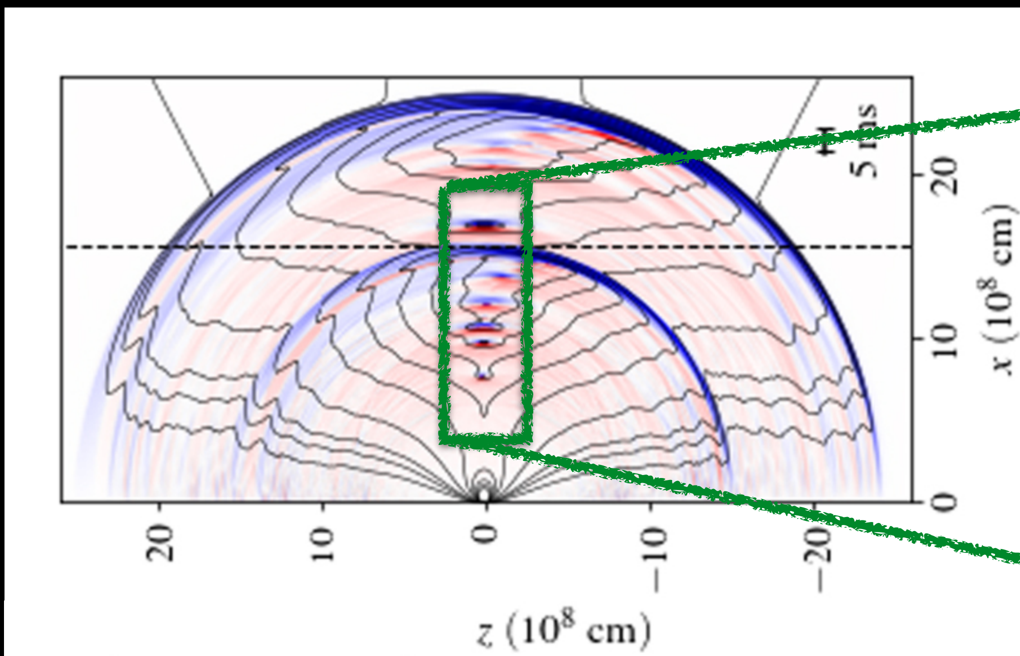

(Yuan+ 20)

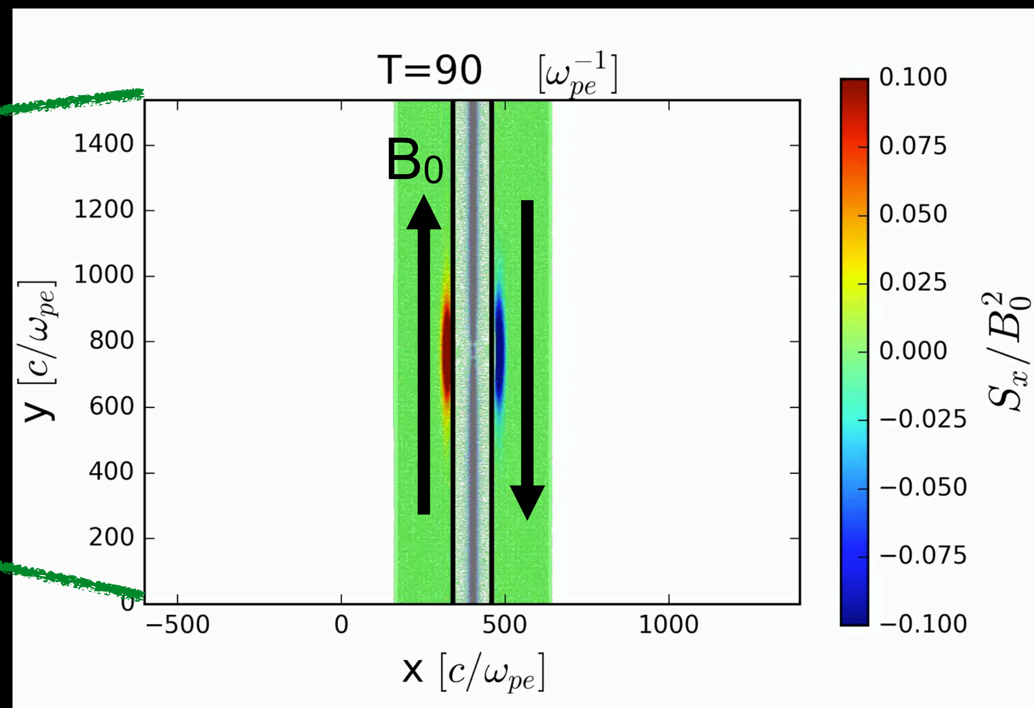

(credit: N. Sridhar)

- Plasmoid mergers produce fast magnetosonic waves, which can escape as vacuum e.m. waves.

- Invoked for pulsar giant radio pulses (Lyubarsky 19, Philippov+ 19).

Relativistic shocks from magnetar flares

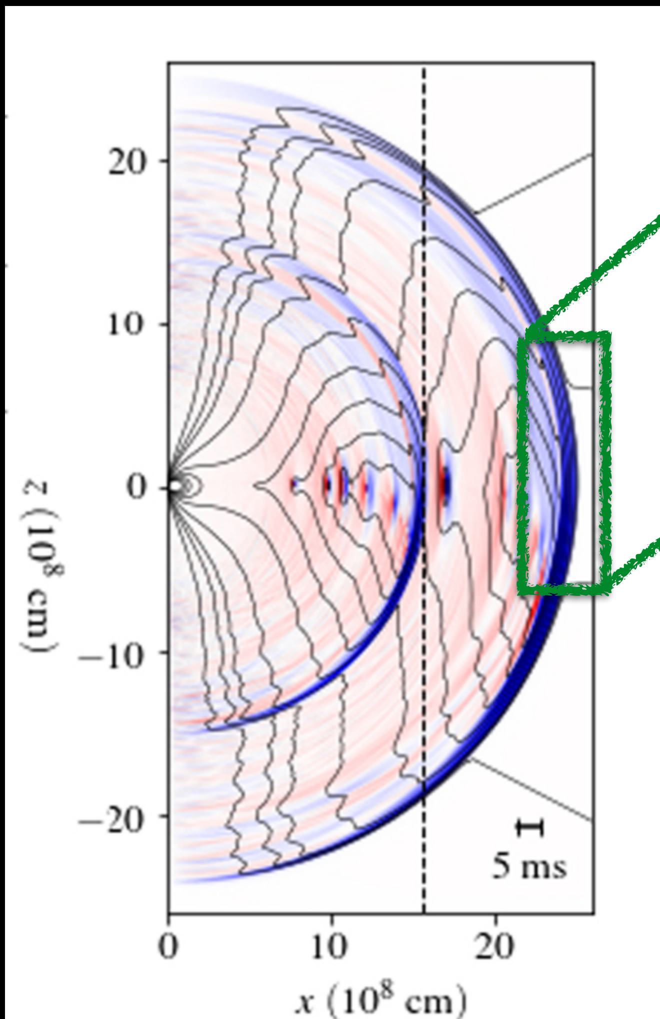

(Yuan+ 20)

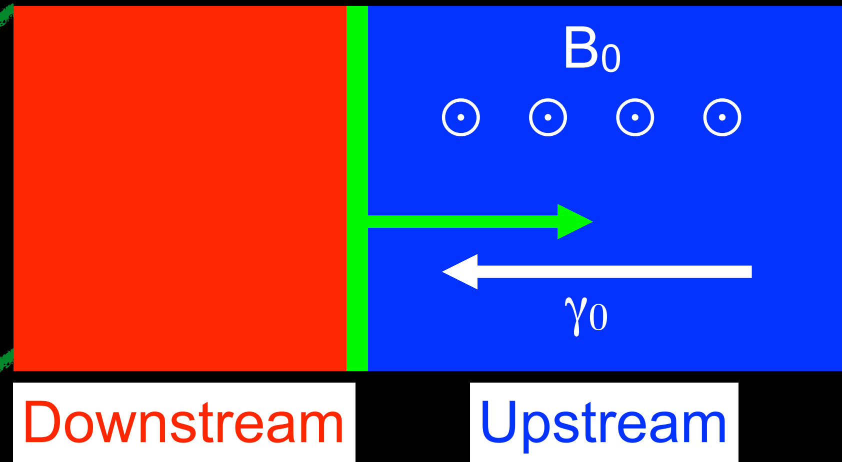

- Ultra-relativistic: Lorentz factor $\gamma_0 \gg 1$
- Magnetized: $\sigma \gtrsim 1$ (possibly $\sigma \gg 1$)

$$\sigma = \frac{B_0^2}{4\pi\gamma_0\rho c^2}$$

- Transverse or "perpendicular"
- Pre-shock medium:
  - magnetar e^-e^+ wind, or
  - $e^-e^+p^+$ shell ejected in a prior flare (Iwamoto's talk)

Studying the mechanism: the PIC method

Particle-in-Cell (PIC) method:

It is the <u>most fundamental way</u> of capturing the interplay of charged particles and electromagnetic fields, with *no assumptions*.

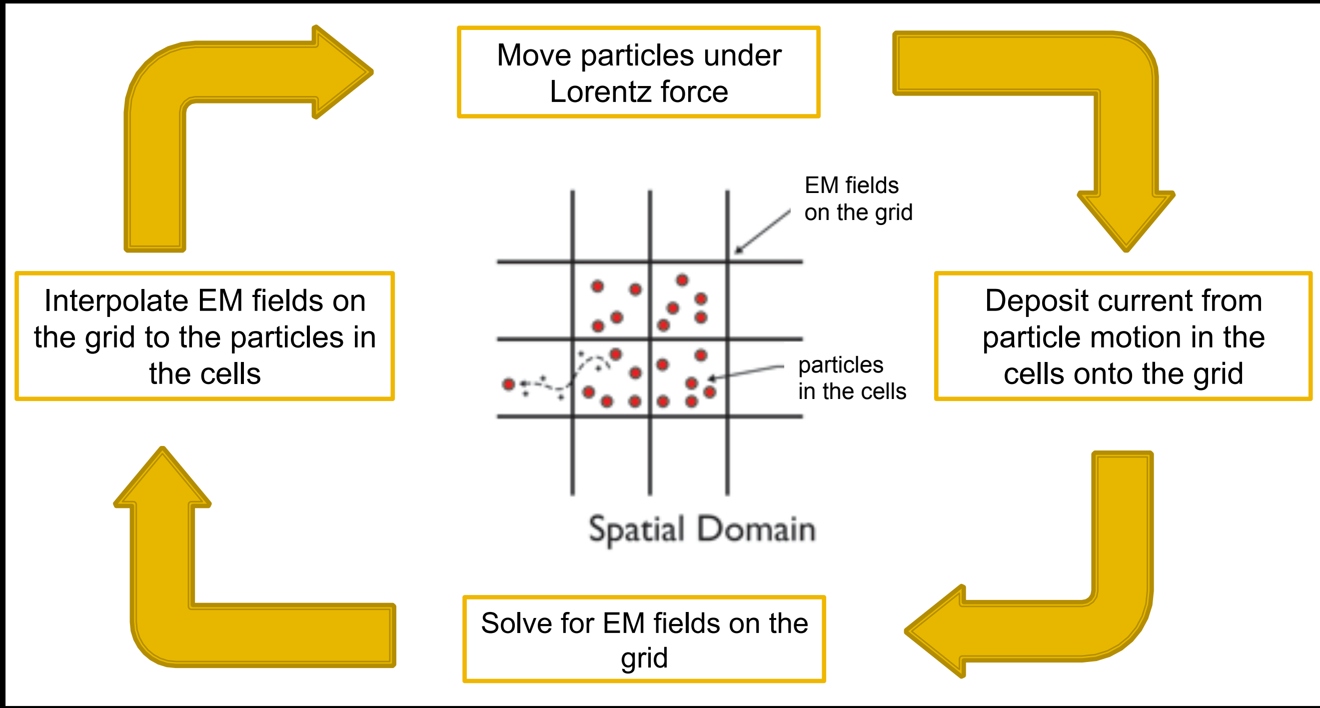

The computational challenge:

The *microscopic* scales resolved by PIC simulations are much smaller than *astronomical* scales.

Typical length (c/ω_p) and time ($1/\omega_p$) scales are:

$$\frac{c}{\omega_p} \simeq 5.5\times 10^5 \left(\frac{n}{1\,\mathrm{cm}^{-3}}\right)^{-1/2} \mathrm{cm} \qquad \frac{1}{\omega_p} \simeq 1.8\times 10^{-5} \left(\frac{n}{1\,\mathrm{cm}^{-3}}\right)^{-1/2} \mathrm{s}$$

$$\omega_p = \omega_{pe} \quad ; \quad \omega_{pi} = \omega_{pe}\sqrt{m_e/m_i}$$

FRBs are not GRBs

- GRB (low-σ) shocks: accelerated particles → filamentation instabilities

σ=0
γ_0=15
e^--e^+

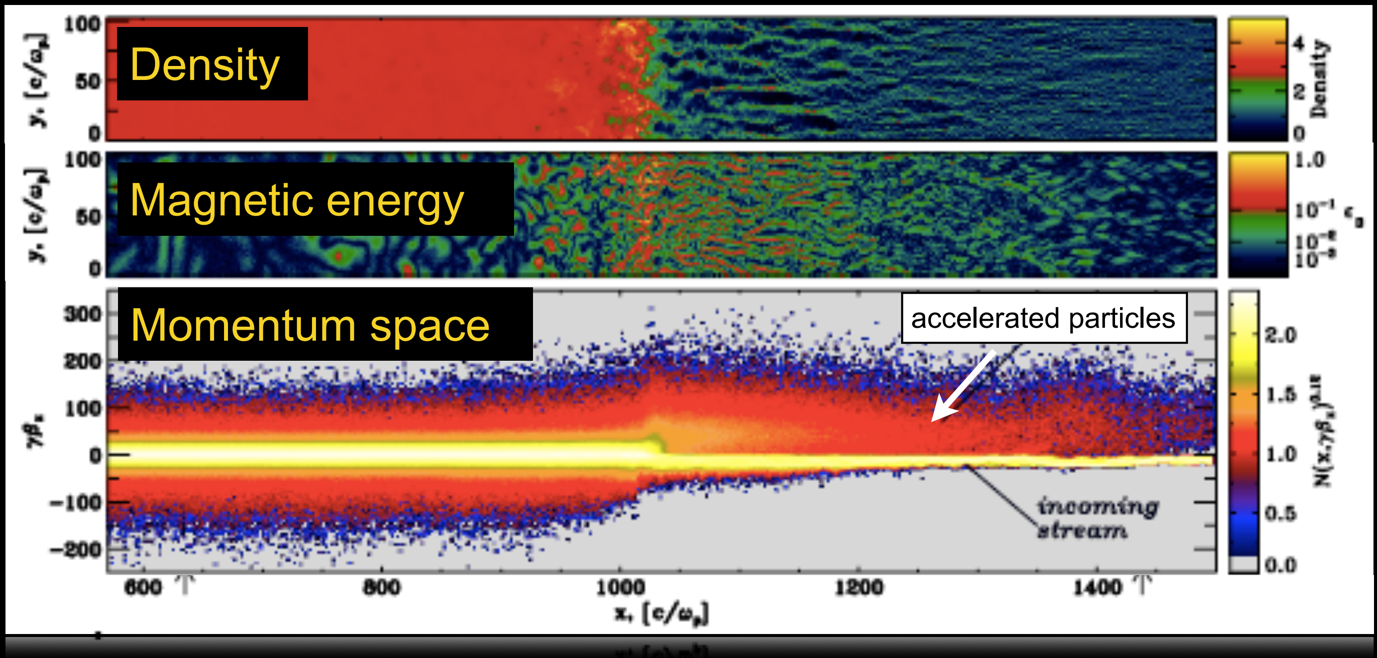

(LS et al 13)

- FRB (high-σ) shocks: no accelerated particles → no turbulence

σ=0.1
perp shock
γ_0=15
e^--e^+

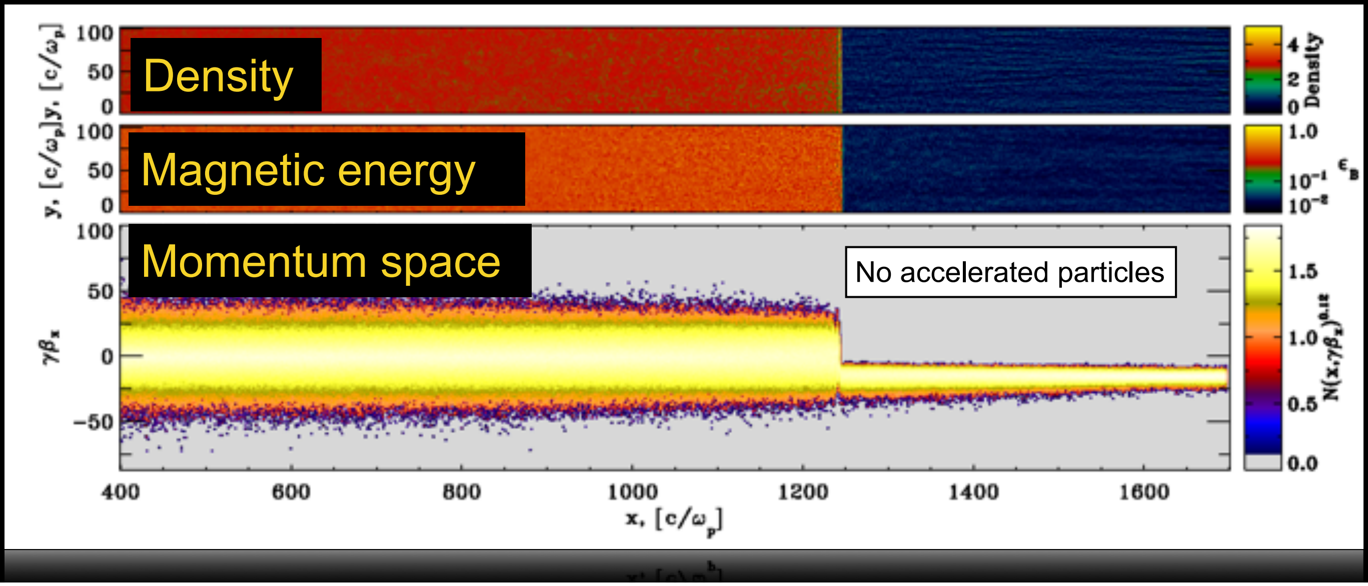

(LS & Spitkovsky 11)

The synchrotron maser

The synchrotron maser:

(1) Electrons and positrons gyrate *coherently* in the shock field.

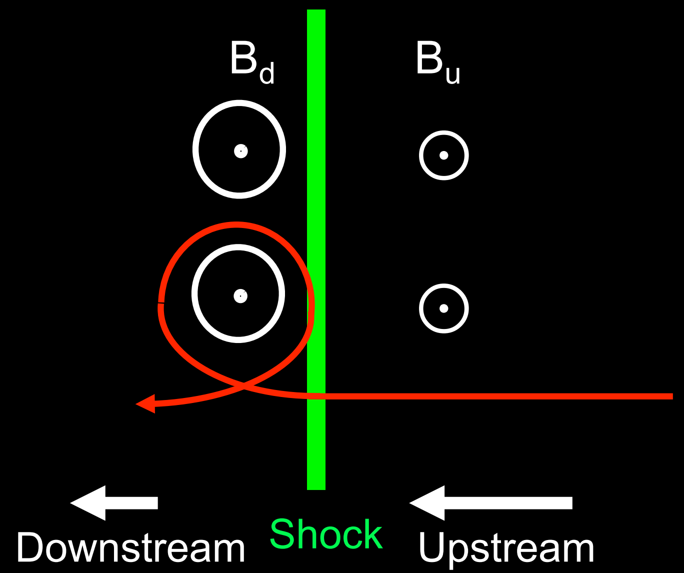

The synchrotron maser

The synchrotron maser:

(1) Electrons and positrons gyrate *coherently* in the shock field.

(2) Shocked particles form an unstable "ring" distribution in momentum space.

The population inversion is constantly replenished.

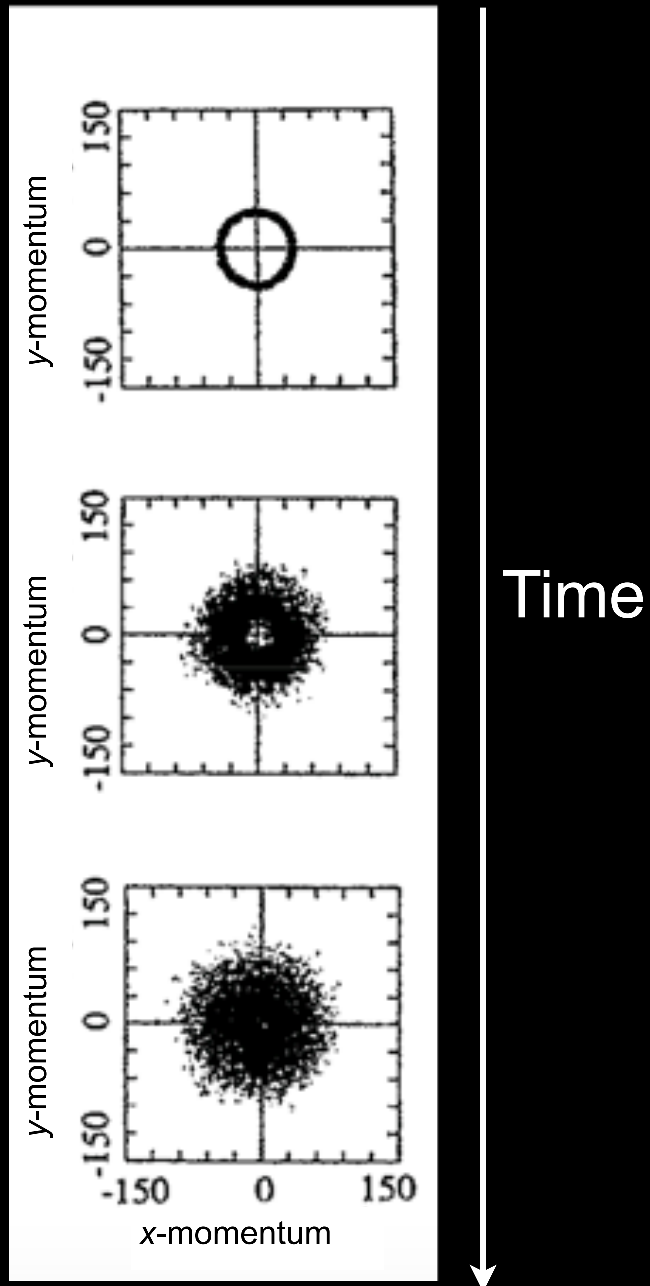

(Hoshino & Arons 91)

The synchrotron maser

The synchrotron maser:

(1) Electrons and positrons gyrate *coherently* in the shock field.

(2) Shocked particles form an unstable "ring" distribution in momentum space.

The population inversion is constantly replenished.

(3) Collapse of the unstable ring results in the emission of e.m. "precursor" waves.

→ FRBs [?] from first principles!

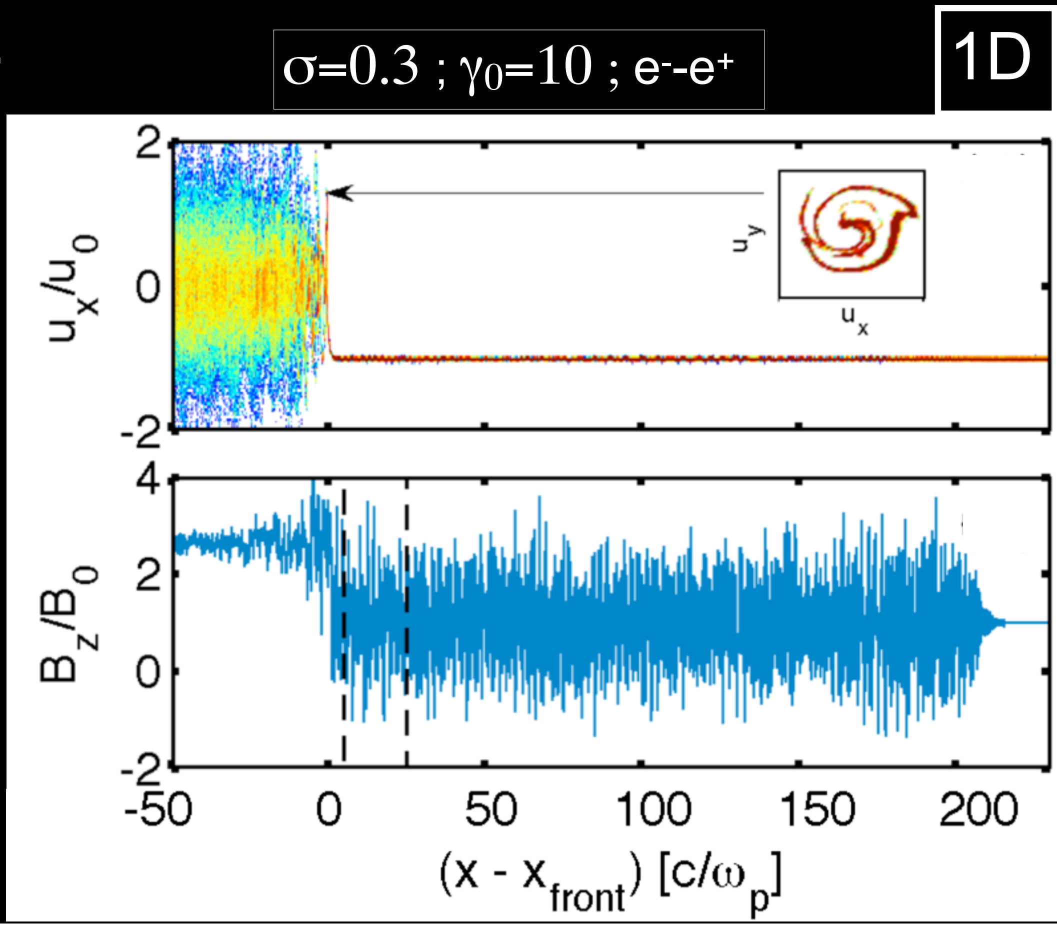

(Plotnikov & LS 19)

Shock-powered coherent emission

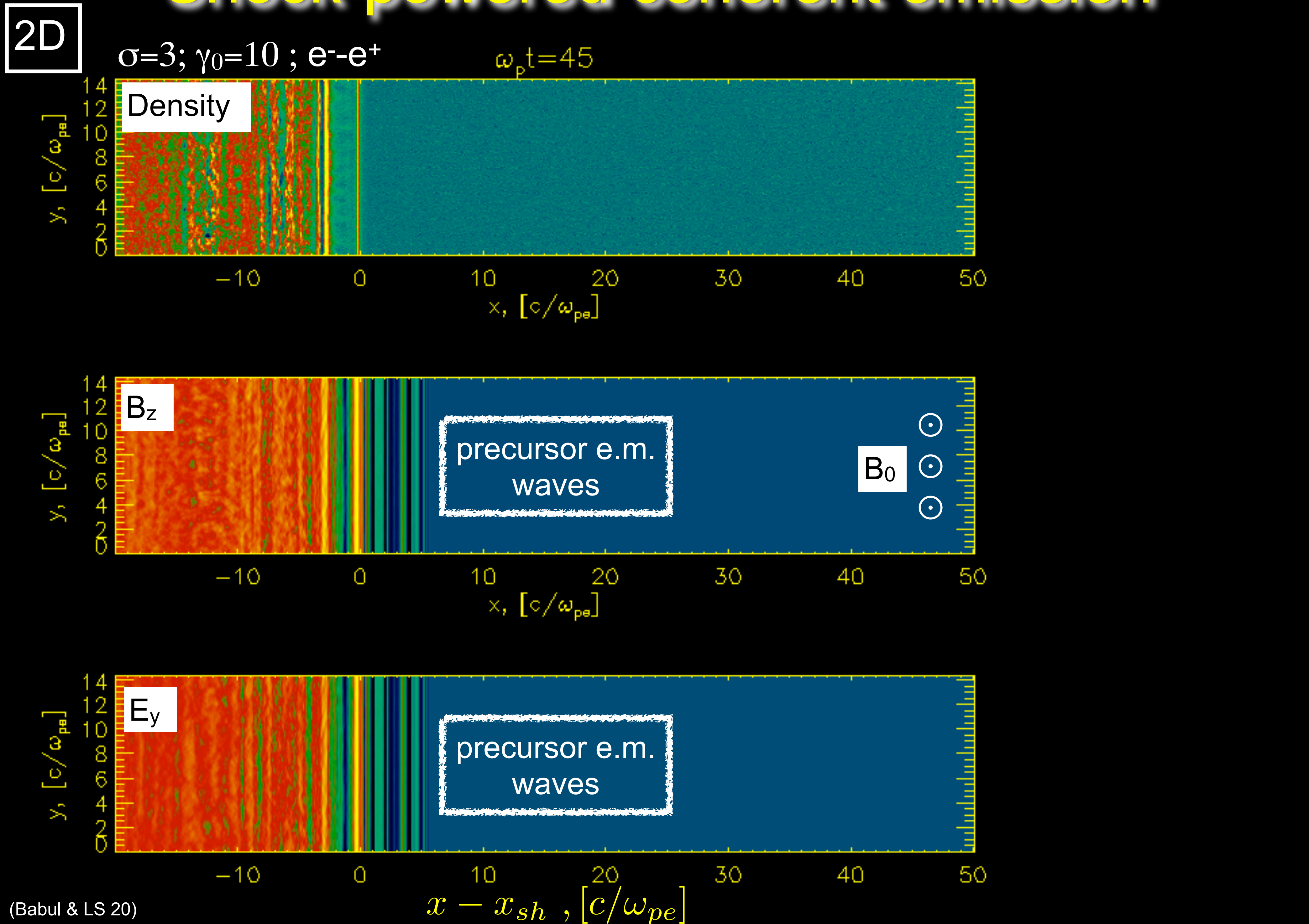

(Babul & LS 20)

Shock-powered coherent emission

3D

$\sigma=0.6$; $\gamma_0=10$; e^--e^+

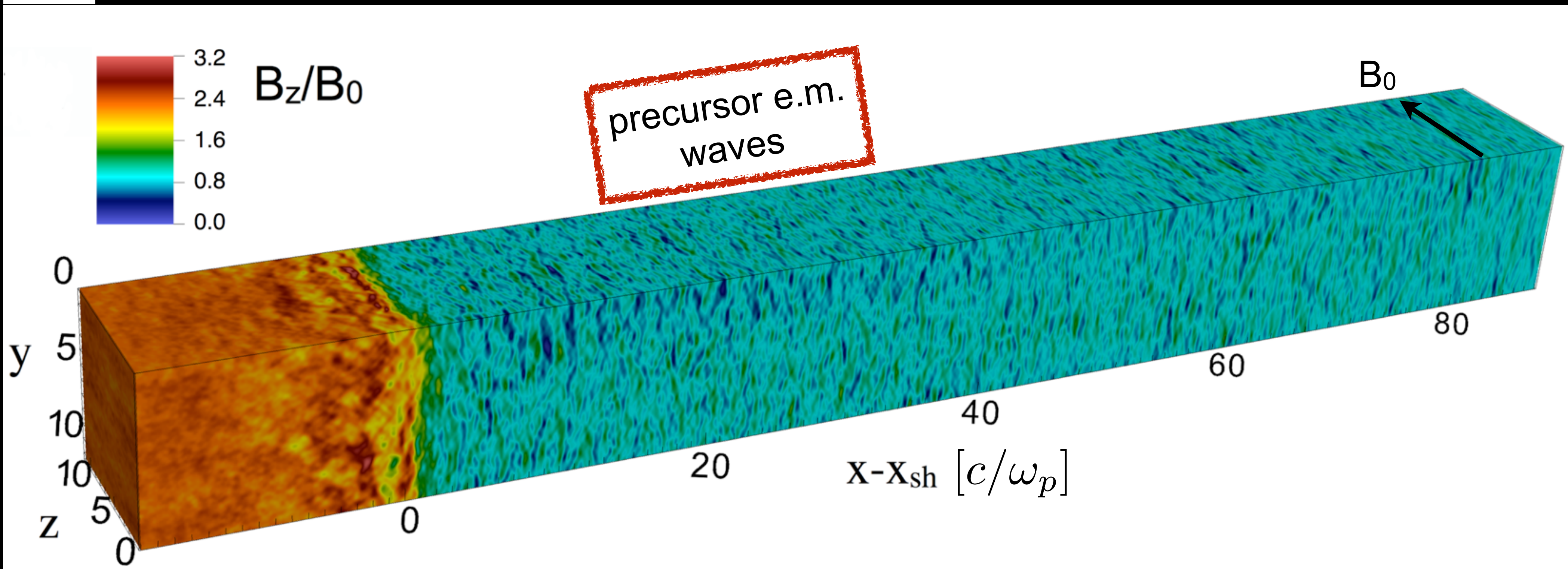

(Nattila, LS+ 21, in prep)

→ Synchrotron maser emission is robust in 1D, 2D, 3D

PIC simulations allow to assess from first principles:

(1) Efficiency

(2) Spectrum

(3) Beaming

(4) Polarization

Preamble: high-σ shocks are fast

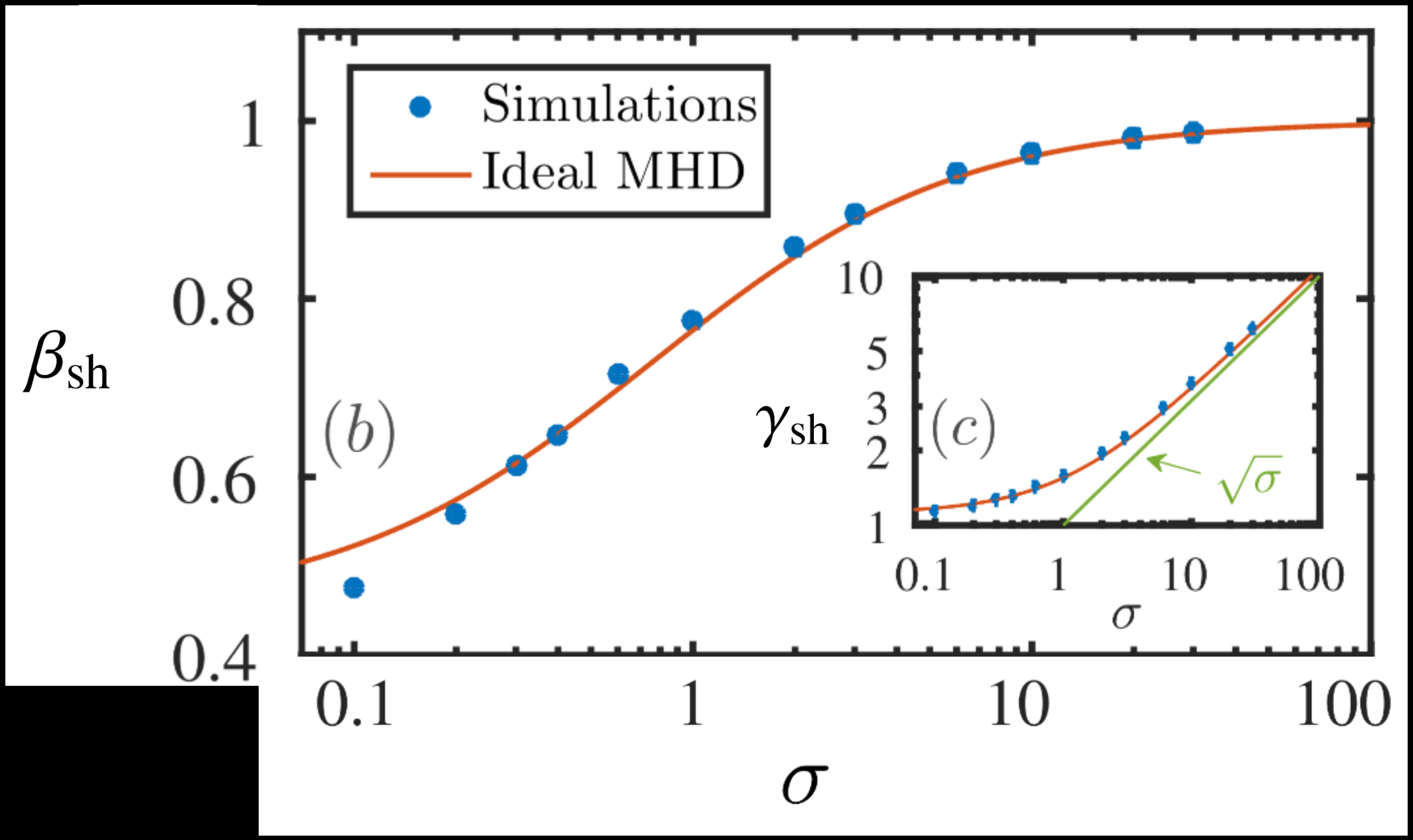

Shock Lorentz factor in post-shock frame: $\gamma_{sh} \simeq \sqrt{\sigma}$

Shock speed in post-shock frame: $\beta_{sh} \simeq 1 - 1/2\sigma$

(1) Efficiency

(1) Efficiency vs magnetization

Dependence on $\sigma = \dfrac{B_0^2}{4\pi\gamma_0\rho c^2}$

γ_0=10

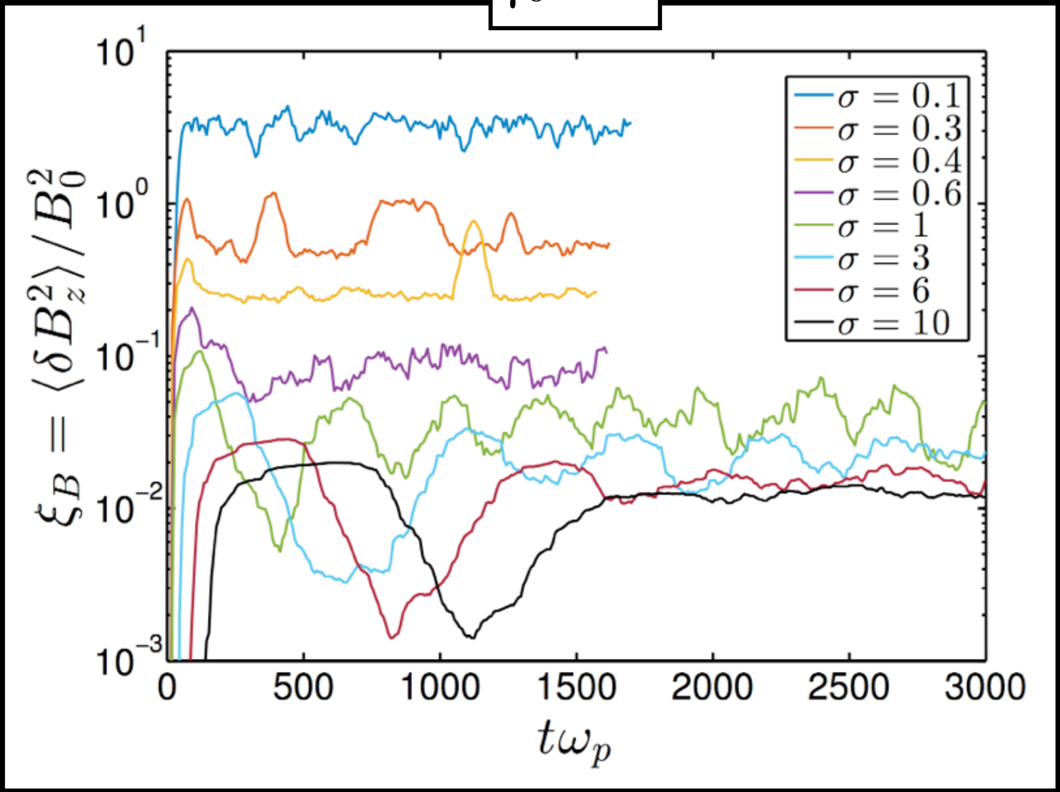

γ_0=10

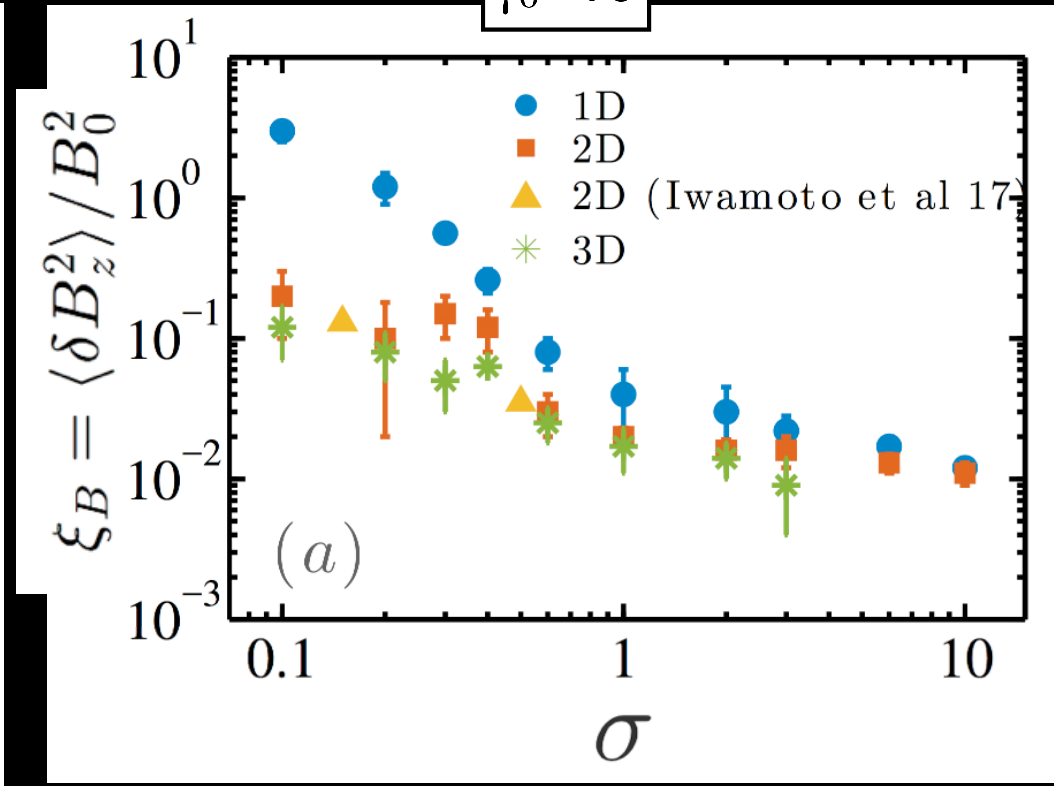

(Plotnikov & LS 19)

The precursor emission reaches a <u>steady state</u>.

Its fractional amplitude $\xi_B = \langle \delta B_z^2 \rangle / B_0^2$ drops for $\sigma \lesssim 1$, it is ~ constant for $\sigma \gtrsim 1$.

(1) Efficiency vs magnetization

Efficiency:

$$f_\xi = \frac{E_{out}}{E_{in}} = \xi_B \left(\frac{\sigma}{1+\sigma}\right)\left(\frac{1-\beta_{sh}}{\beta_0+\beta_{sh}}\right)$$

E_{in}=incoming energy (kinetic+e.m.)

E_{out}=escaping energy (e.m.)

γ_0=10

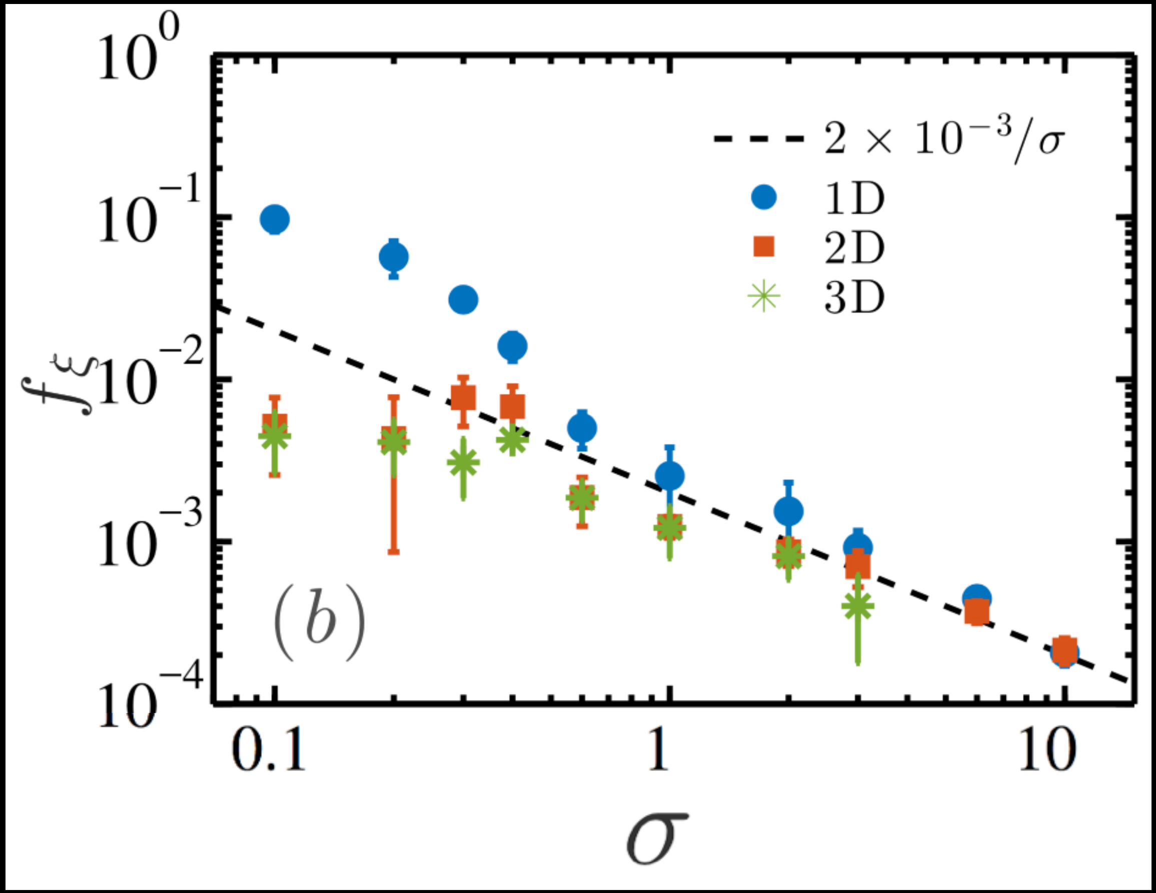

(Plotnikov & LS 19)

- 1D, 2D and 3D give similar efficiencies for $\sigma \gtrsim 1$.
- At high σ, the efficiency drops as $\propto 1/\sigma$.

(1) Efficiency vs temperature

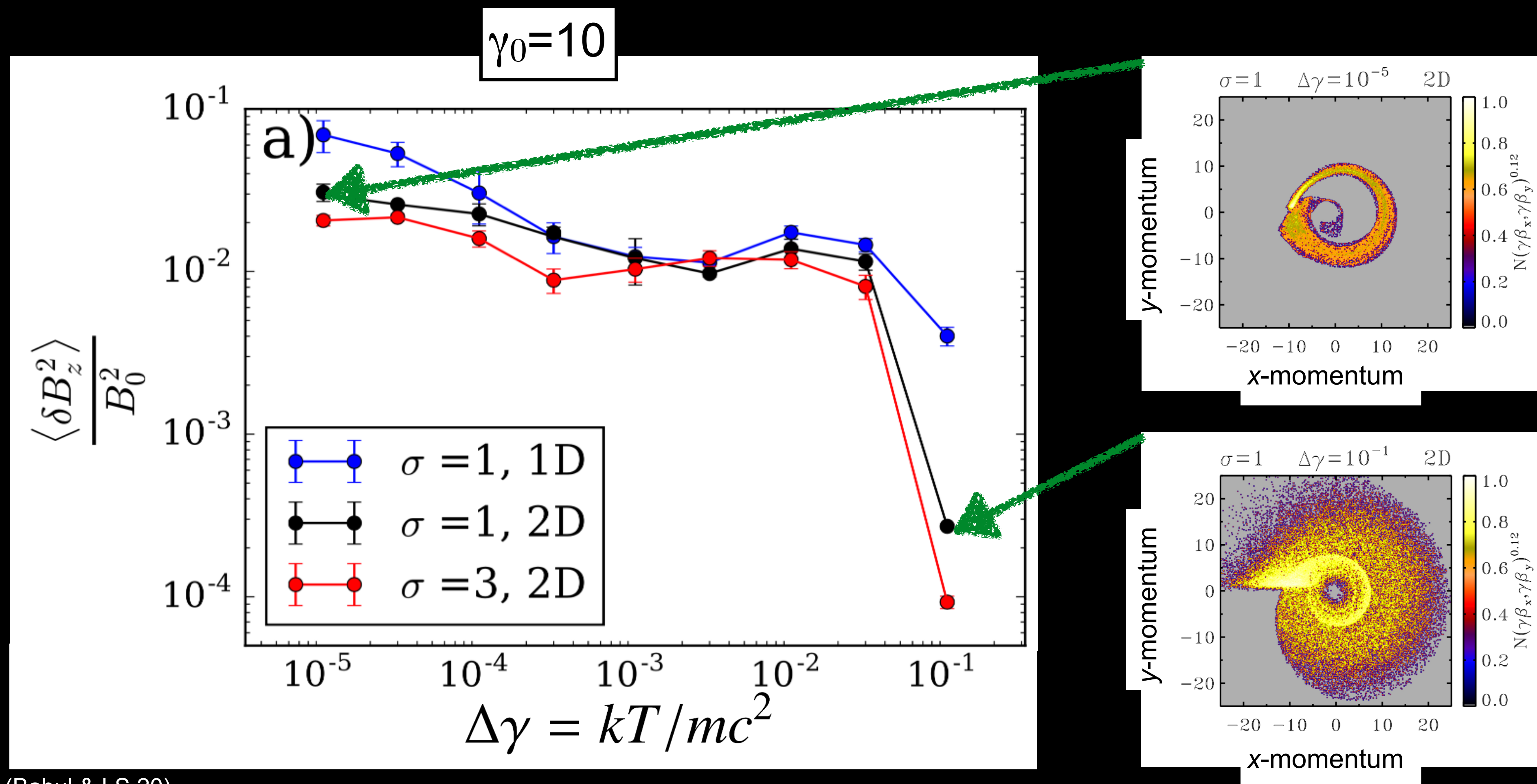

(Babul & LS 20)

Nearly constant efficiency for kT/mc^2 between 10^{-5} and 0.03.

Vanishing efficiency for $kT/mc^2 \gtrsim 0.1$, in both 1D and 2D.

A large <u>longitudinal</u> momentum spread kills the synchrotron maser.

(1) Efficiency vs flow Lorentz factor

Dependence on γ_0

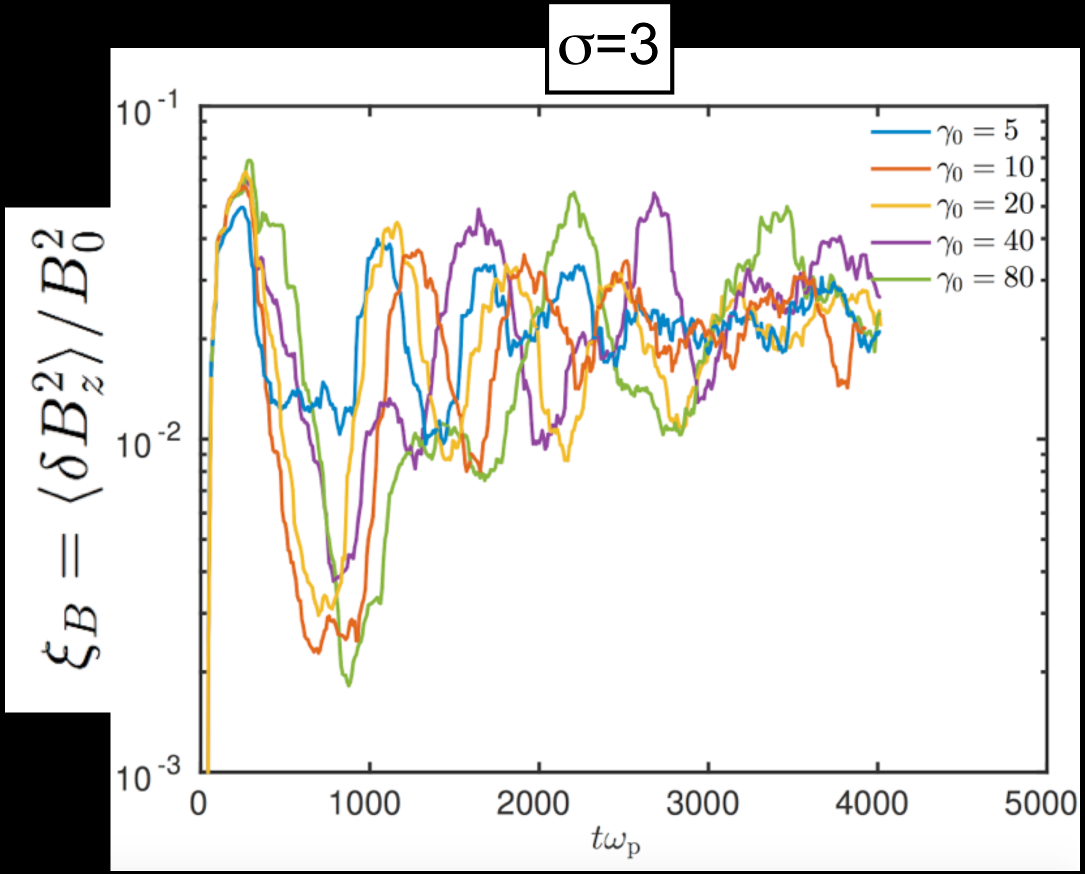

(Plotnikov & LS 19)

The precursor efficiency does not depend on γ_0.

Equivalently, it does not depend on the wave strength

$$a = \frac{e\,\delta B_z}{mc\omega} \sim \sqrt{\xi_B}\,\gamma_0$$

(2) Spectrum

(2) Spectrum vs magnetization

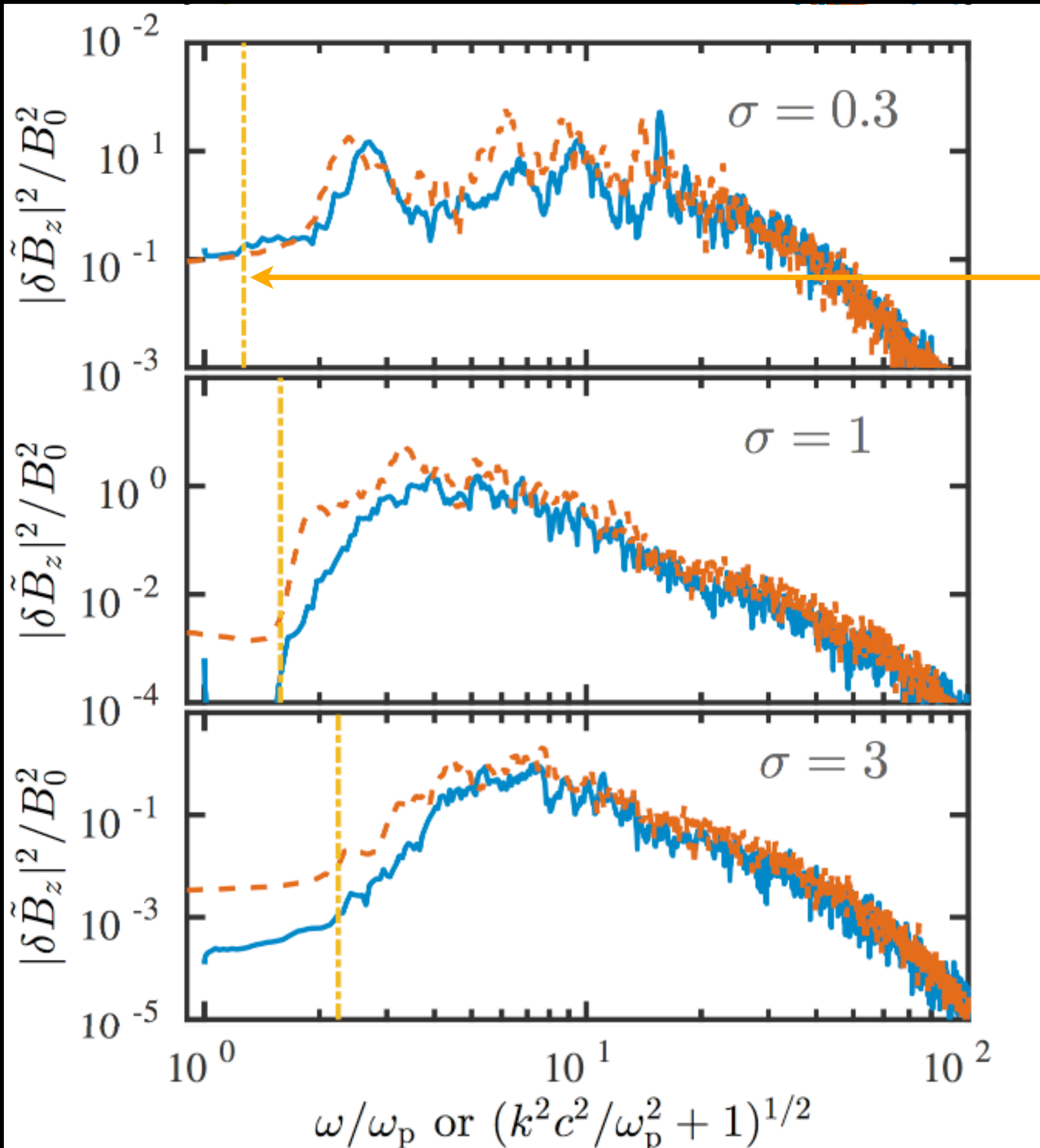

1D, γ_0=10

The shock acts as a high-pass filter:

$$v_{ph}(\omega) = v_{sh}$$

The spectrum peaks at higher frequencies for larger σ.

The fractional spectral width is Δω/ω~1, but with narrower line-like features.

(Plotnikov & LS 19)

The shock cavity

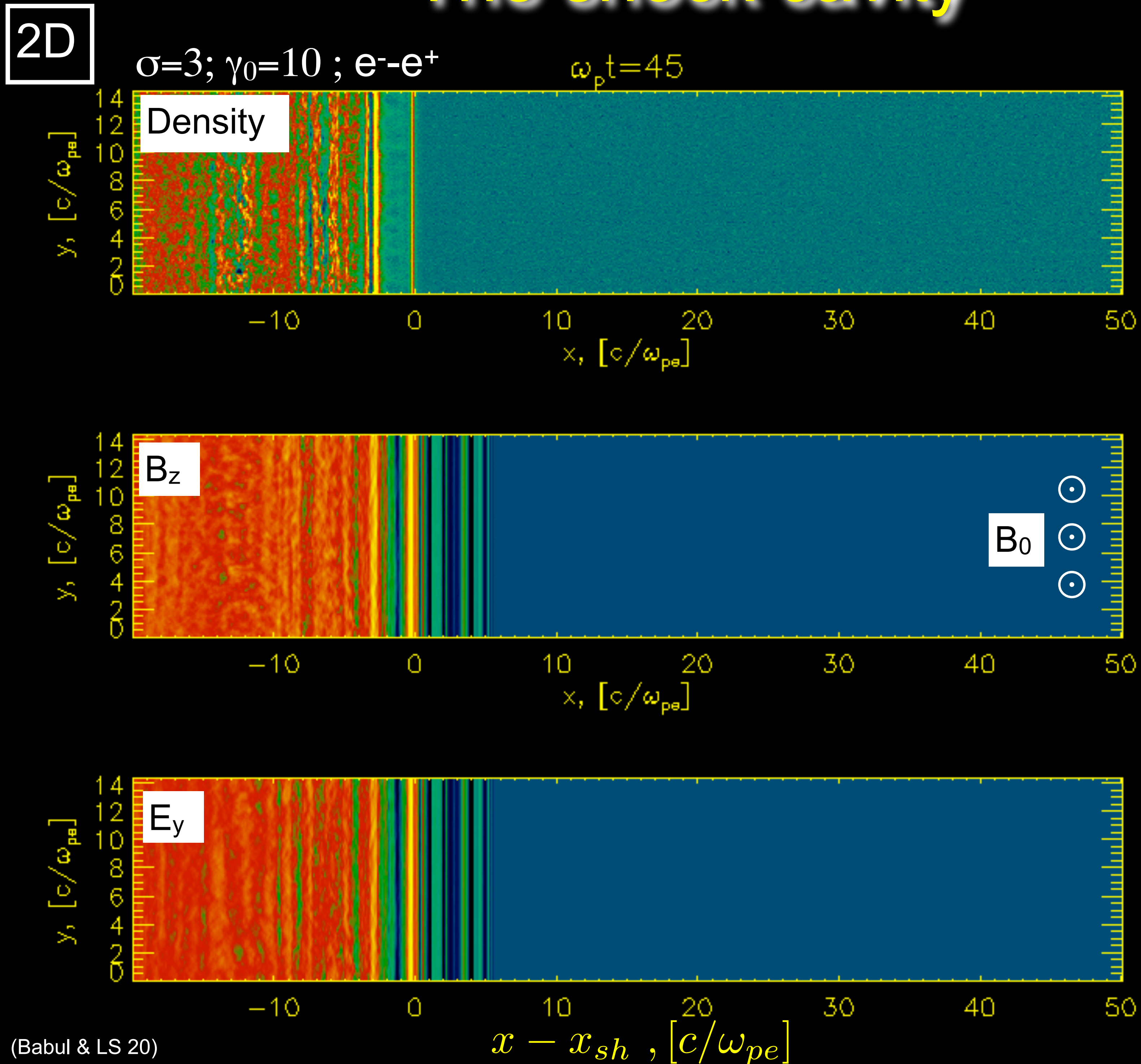

(Babul & LS 20)

(2) The spectral peak

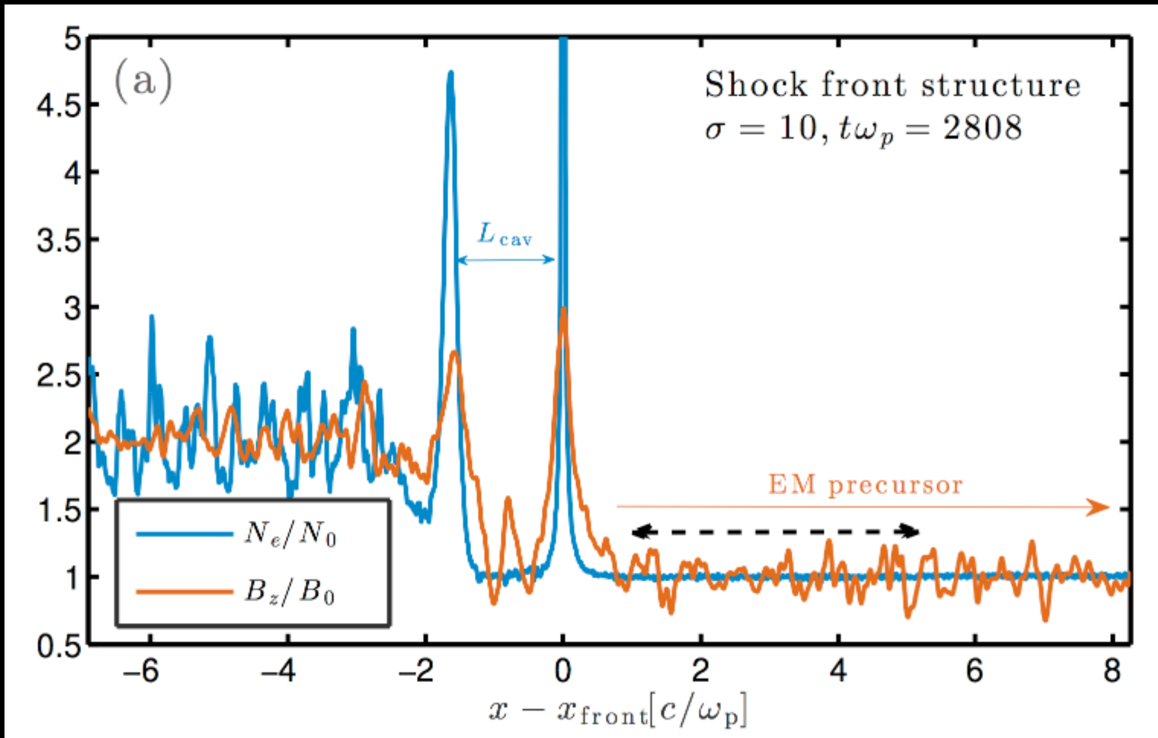

At high σ, the spectral peak is an eigenmode of the shock cavity.

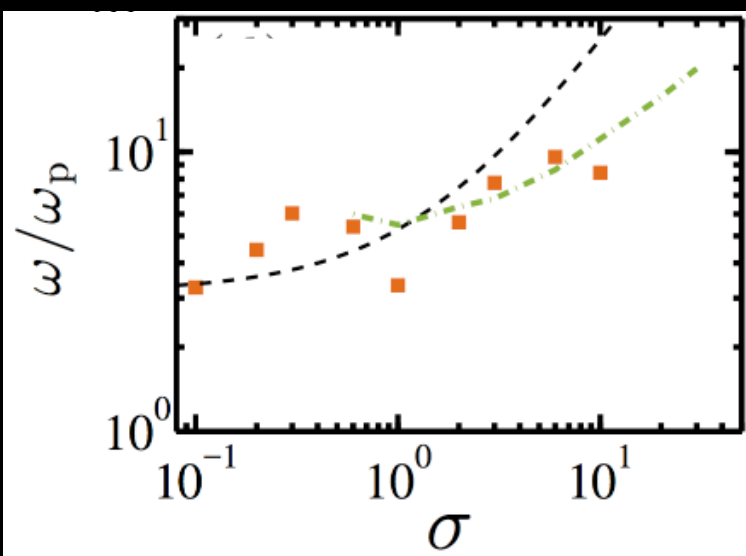

Peak frequency

In post-shock frame, $\omega_{peak} \simeq 3\,\omega_p \max[1, \sqrt{\sigma}]$

In pre-shock (observer) frame, $\omega''_{peak} \approx 3\gamma_{s|u}\omega_p$

(Plotnikov & LS 19)

(2) Spectrum vs temperature

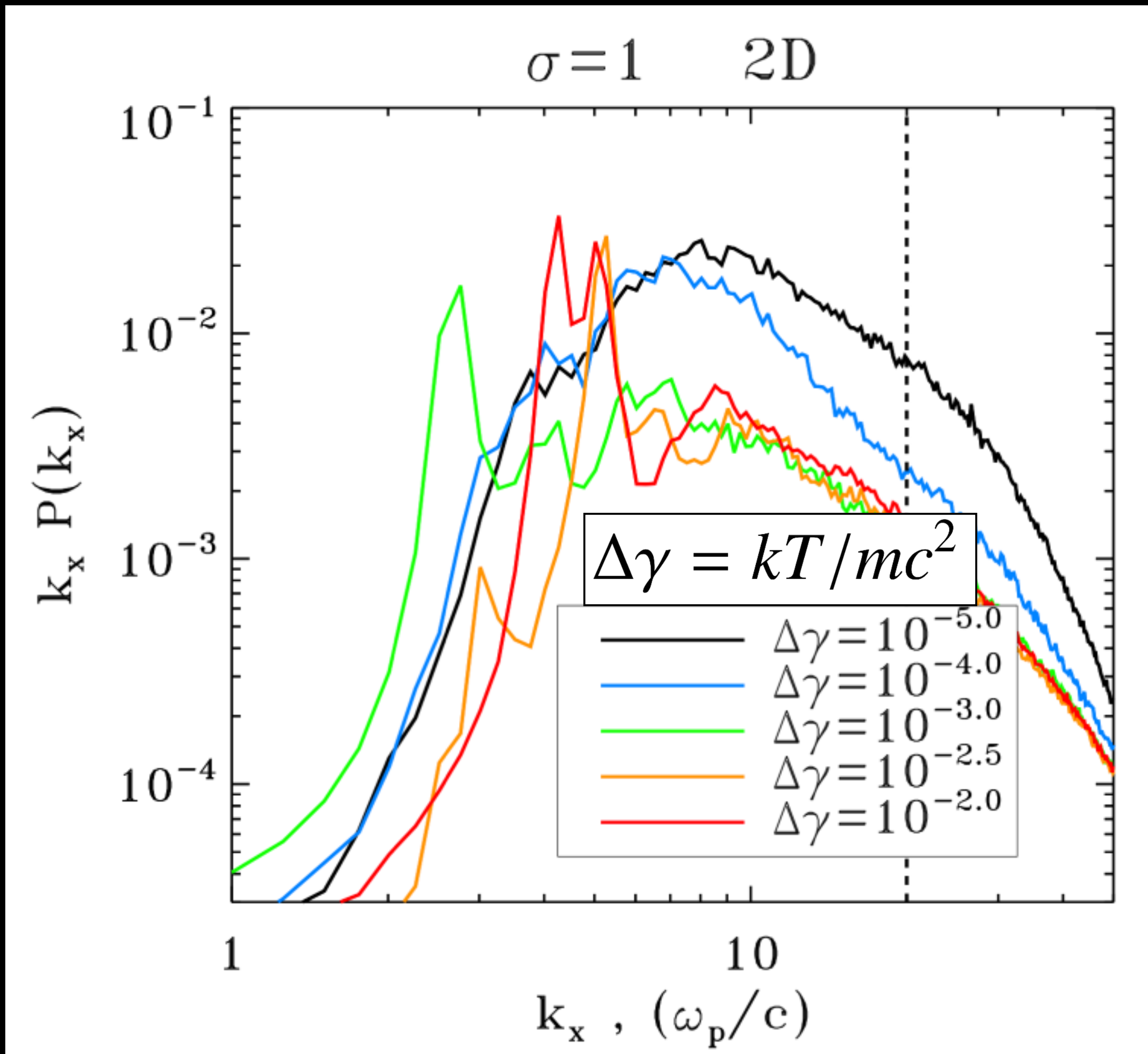

(Babul & LS 20)

For warmer plasmas, less power at high frequencies.

For warmer plasmas, more distinct line-like features.

(3) Beaming

(3) Beaming

The precursor waves can escape ahead of the shock only if

$$k_x \geqslant \gamma_{\rm sh}\beta_{\rm sh}\sqrt{k_y^2 + \frac{\omega_{\rm p}^2}{c^2}}$$

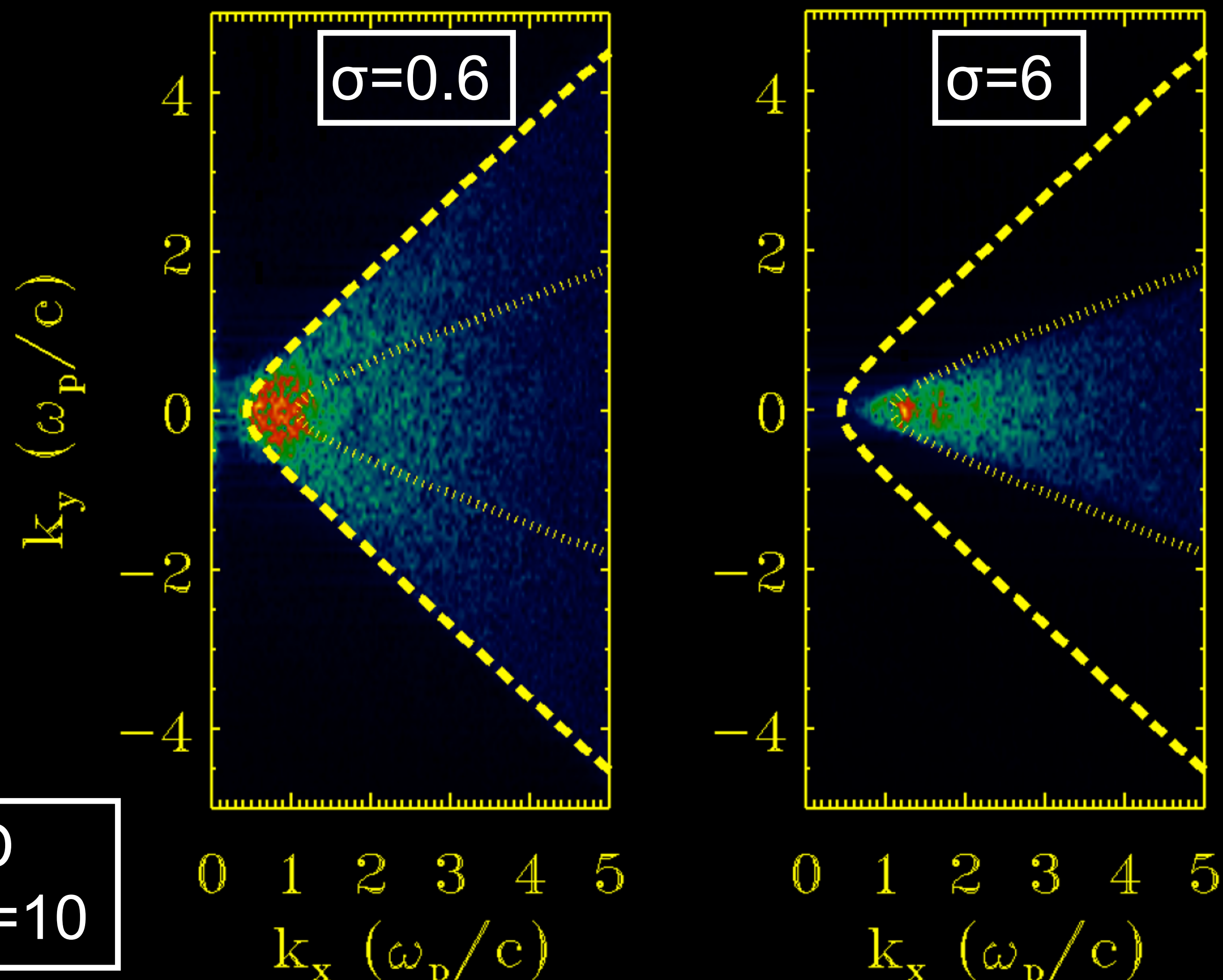

For σ≫1: $\gamma_{\rm sh}\beta_{\rm sh} \simeq \sqrt{\sigma}$

Emission is beamed within an angle

$$\sim 0.7/\sqrt{\sigma}$$

from the shock direction of propagation.

2D
γ_0=10

(Babul & LS 20)

(4) Polarization

(4) Polarization

- In 1D and 2D with out-of-plane $\mathbf{B}_0$:

  Only the X-mode with $\delta\mathbf{B} \,//\, \mathbf{B}_0$ can grow.

  The emission is 100% polarized.

- In 2D with in-plane $\mathbf{B}_0$ and 3D:

  Also the O-mode with $\delta\mathbf{B} \perp \mathbf{B}_0$ can be generated.

  This may decrease the degree of linear polarization.

(4) Polarization

3D

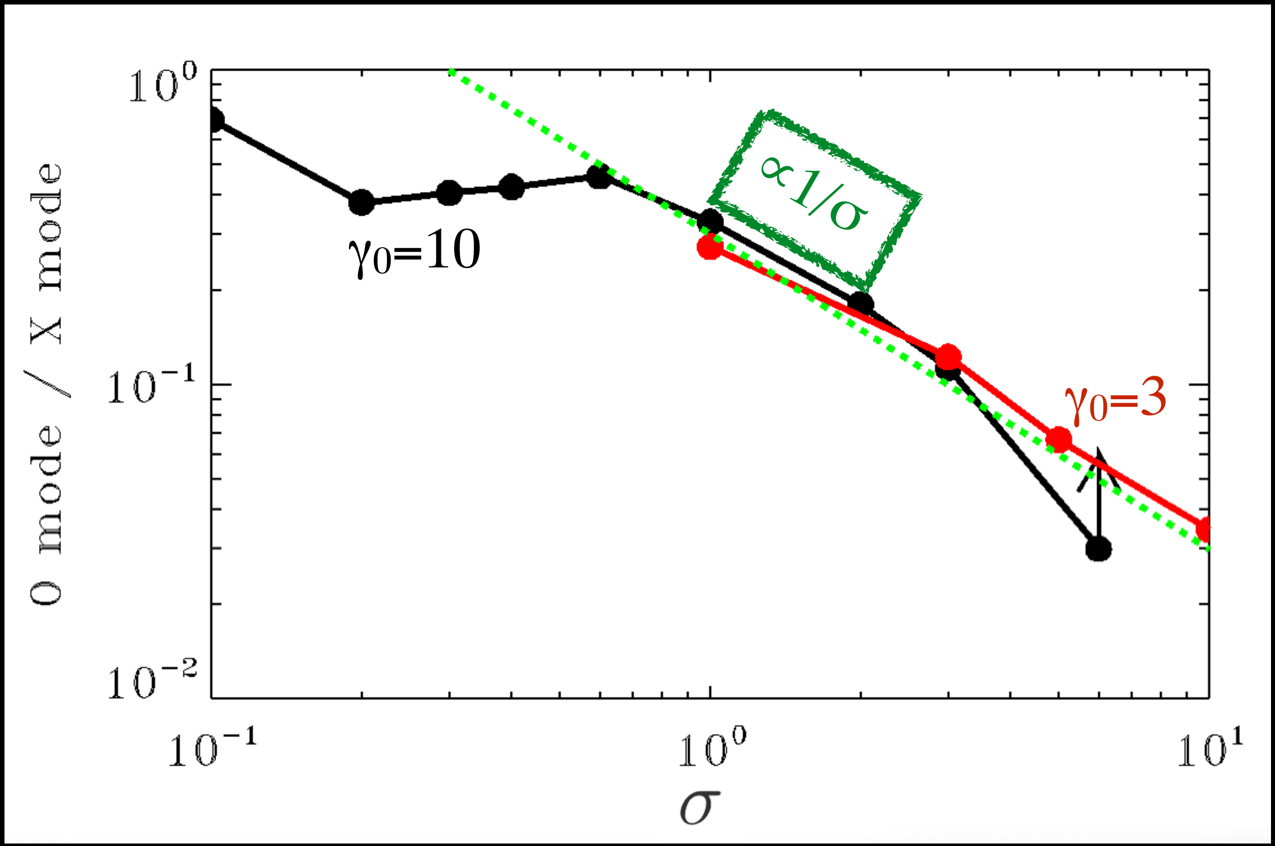

(Nattila, LS+ 21, in prep)

$$PD = 1 - \frac{O-\text{mode}}{X-\text{mode}}$$

- The polarization degree (PD) increases with σ.
- We expect >99% linear polarization for σ≳30.

Implications for FRBs:

(1) Efficiency

In cold plasmas, $f_\xi \sim 10^{-3}\,\sigma^{-1}$
→ constraints on the energetics of the FRB engine.

Much lower efficiency in hot plasmas, if $kT/mc^2 \gtrsim 0.1$
→ constraints on the "lag time" between consecutive FRBs.

(2) Spectrum

In cold plasmas, broad spectrum peaking at $\omega''_{\rm peak} \approx 3\gamma_{\rm s|u}\omega_{\rm p}$
→ downwards frequency drift as the shock decelerates.

Line-like features in warm plasmas.
→ FRB sub-pulses may be due to lines drifting into the observing band.

Implications for FRBs:

(3) Beaming

Shock Lorentz factor at high σ is $\gamma_{\rm sh} \simeq \sqrt{\sigma}$

→ FRB duration shrinks by an extra 1/σ.

Emission is beamed within $\sim 0.7/\sqrt{\sigma}$ around the shock normal

→ Doppler transformation does not smear out narrow spectral features.

(4) Polarization

Emission is highly polarized with $\mathrm{PD} \simeq 1 - \dfrac{0.3}{\sigma}$

→ preference for high σ.

Polarization vector is dependent on pre-shock field orientation.

Wave generation
①
Wave impact
③

The time-frequency structure of FRB 121102

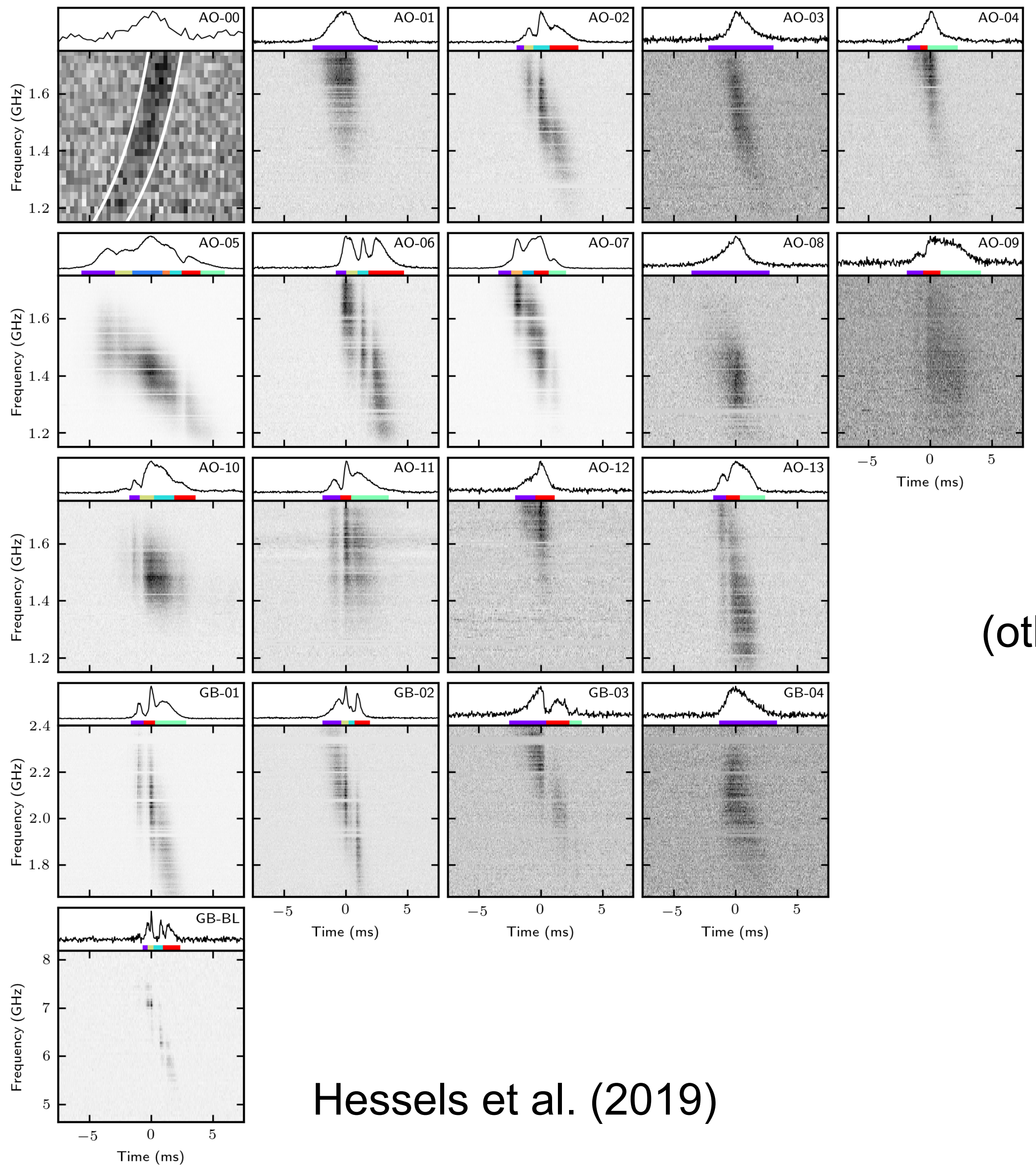

Hessels et al. (2019)

Frequency modulation
with 100-400 MHz bandwidth
(not produced by
diffractive interstellar scintillation)

Sub-bursts
with 0.5-1 ms duration
(other FRBs show 0.01 ms sub-bursts)

What is producing
the time-frequency structure?

Non-linear propagation effects in FRBs

If electrons are non-relativistic,
the propagation of e.m. waves in plasmas is a linear problem described by the dispersion relation

$$\omega^2 = c^2 k^2 + \omega_{\rm P}^2$$

The electron velocity in the electromagnetic field of the wave is a fraction

$$a_0 = \frac{eE}{2\pi \nu m c}$$

of the speed of light.

In typical FRBs, the electron velocity is relativistic close to the source:

$$a_0 \sim 0.2 \left(\frac{\nu}{\rm GHz}\right)^{-1} \left(\frac{L}{10^{42}\ {\rm erg\ s^{-1}}}\right)^{1/2} \left(\frac{R}{10^{14}\ {\rm cm}}\right)^{-1}$$

Non-linear propagation effects are important close to the source!

Self-modulation

Self-modulation is a classical non-linear propagation effect
It has been extensively studied in laser-plasma interaction (e.g. Mourou et al. 2006)

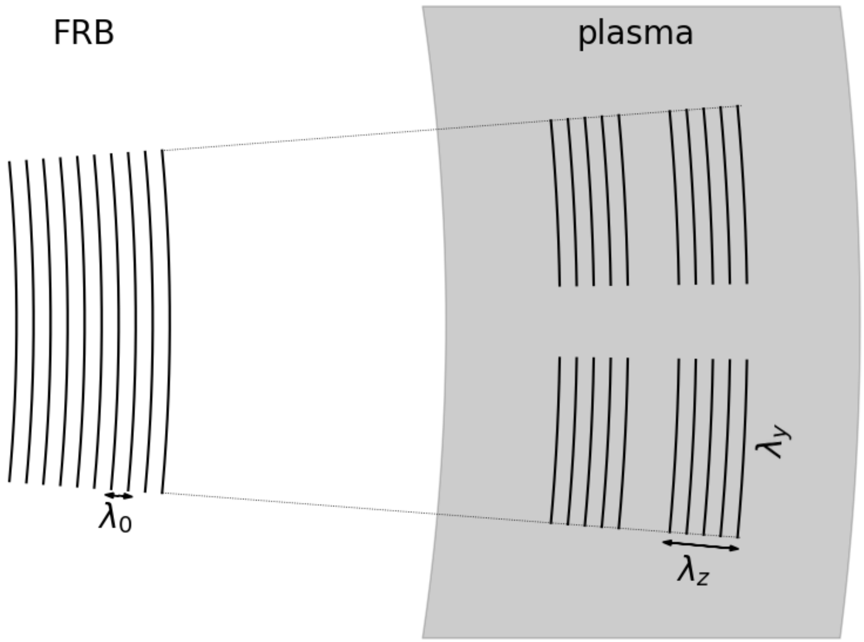

Non-linearity due to
increase of the effective electron mass
in regions with high radiation intensity.

The refraction index increases.

This effect creates a converging lens,
which further increases
the intensity of radiation.

Modulations in the transverse direction

Self-modulation

Self-modulation is a classical non-linear propagation effect
It has been extensively studied in laser-plasma interaction (e.g. Mourou et al. 2006)

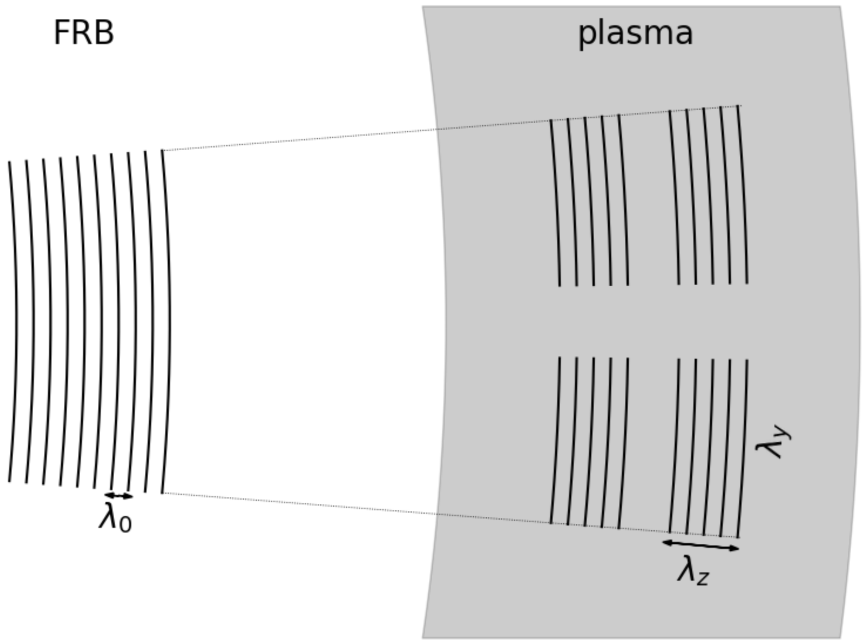

Non-linearity due to
increase of the effective electron mass
in regions with high radiation intensity.

The refraction index increases.

The group velocity depends on the
radiation intensity.

Modulations in the longitudinal direction

Self-modulation

Self-modulation is a classical non-linear propagation effect
It has been extensively studied in laser-plasma interaction (e.g. Mourou et al. 2006)

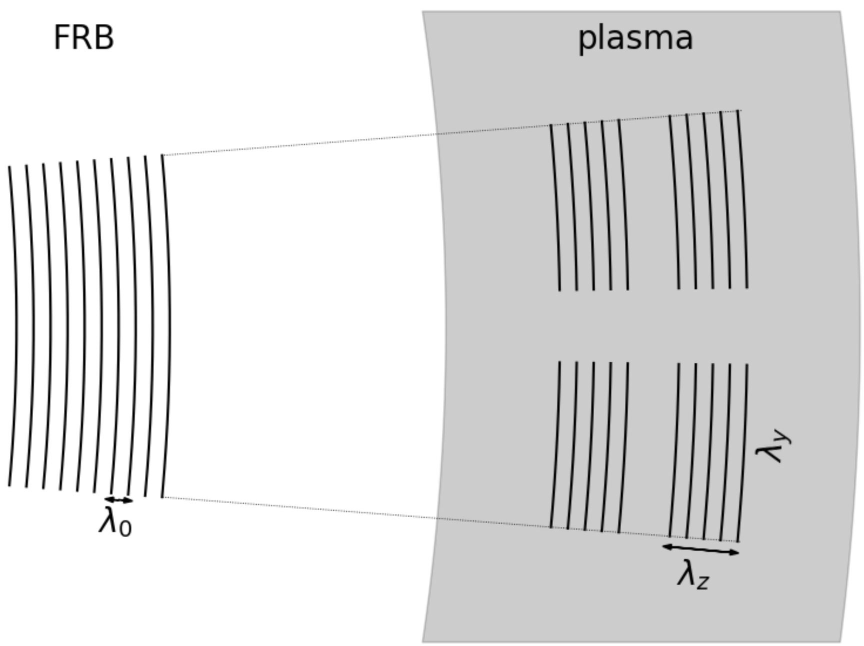

Self-modulation breaks the burst into pancakes

(instability growth rate) x (light crossing time of the plasma slab) > 1

$$R \lesssim R_{\rm crit} \sim 10^{17} \left(\frac{\nu}{\rm GHz}\right)^{-3} \left(\frac{N}{10^2\ {\rm cm^{-3}}}\right) \left(\frac{L}{10^{42}\ {\rm erg\ s^{-1}}}\right)\ {\rm cm}$$

Frequency structure

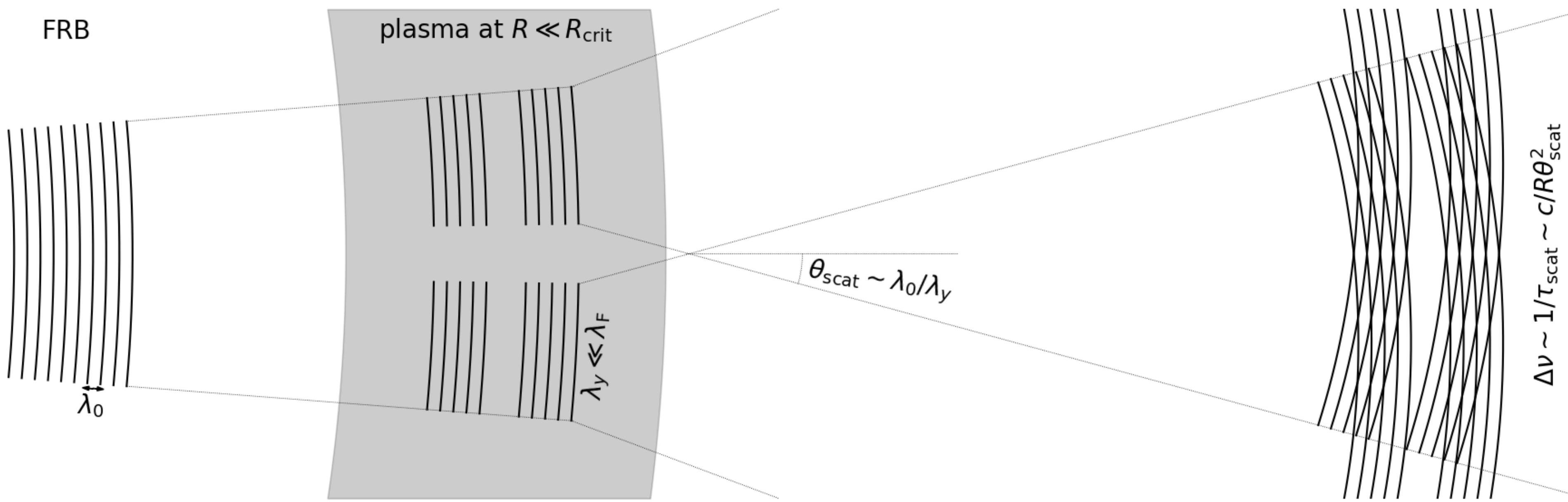

$$\theta_{\rm scat} \sim \frac{\lambda_0}{\lambda_y} \gg \frac{\lambda_y}{R} \sim \theta_{\rm sph}$$ → multi-path propagation

frequency modulation bandwidth ~ 1/(scattering time):

$$\Delta\nu \sim 0.6 \left(\frac{\nu}{\rm GHz}\right)\left(\frac{R}{R_{\rm crit}}\right)\ {\rm GHz}$$

Time structure

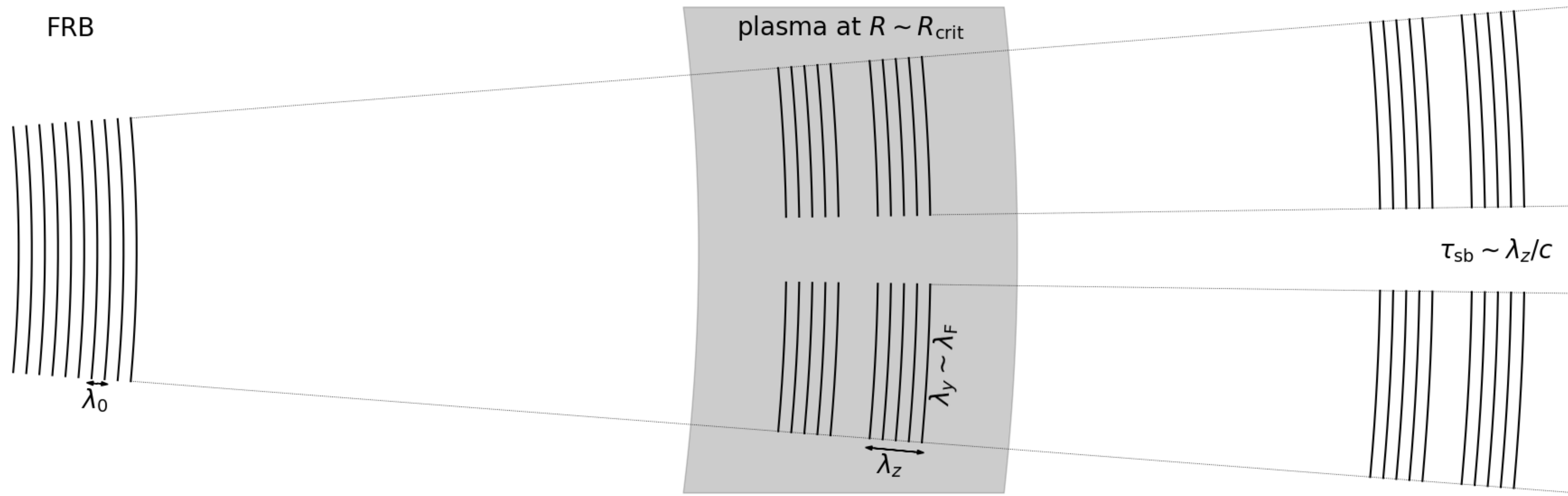

$$\theta_{\rm scat} \sim \frac{\lambda_0}{\lambda_y} \sim \frac{\lambda_y}{R} \sim \theta_{\rm sph}$$ → time structure survives

sub-burst duration ~ (longitudinal wavelength)/c ~ 1/(plasma frequency):

$$\tau_{\rm sb} \sim 10 \left(\frac{N}{10^2 \ {\rm cm}^{-3}} \right)^{-1/2} \ \mu{\rm s}$$

[redacted]

Self-focusing

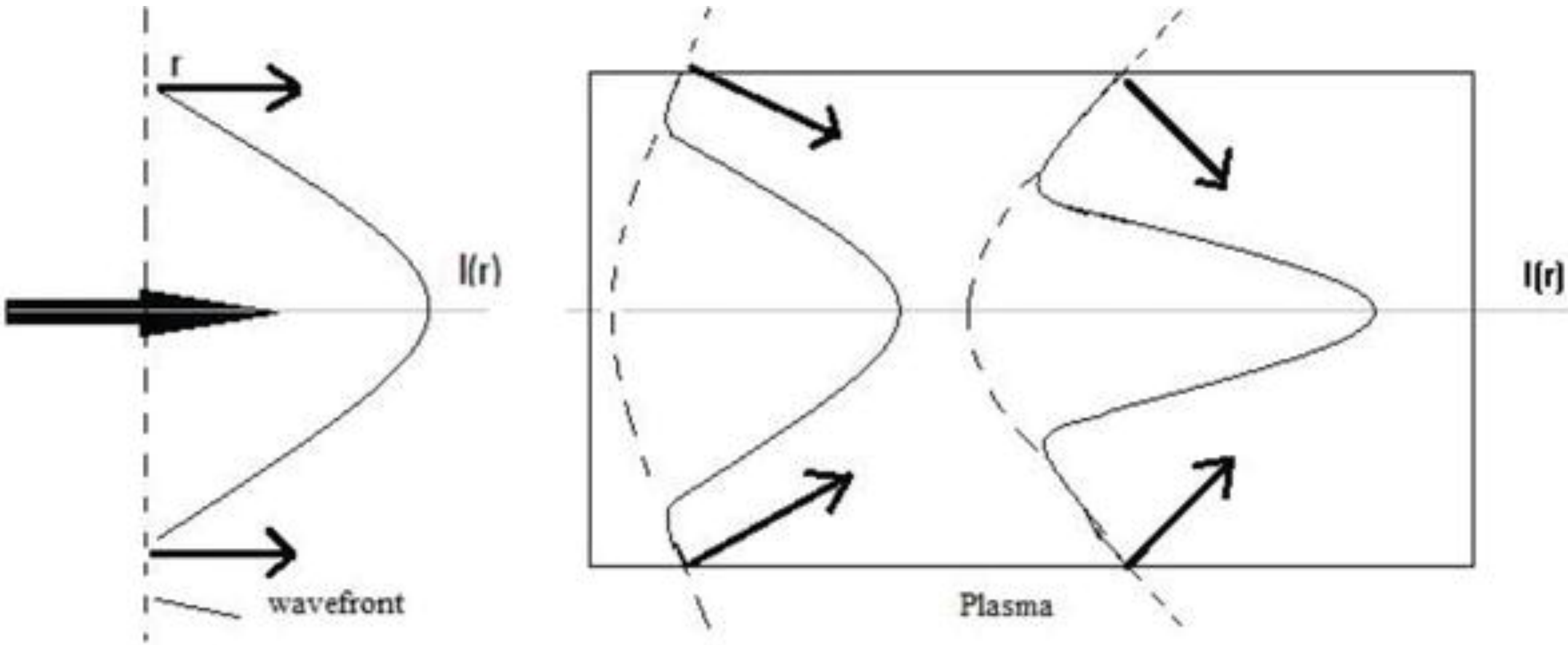

$$n = \sqrt{1 - \frac{\omega_P^2}{\omega^2}} \qquad \omega_P = \sqrt{\frac{4\pi n e^2}{m_{\text{eff}}}}$$

The effective mass increases in regions with high radiation intensity (electrons move faster)

↓

The refraction index increases

↓

Converging lens

Electron-proton shocks

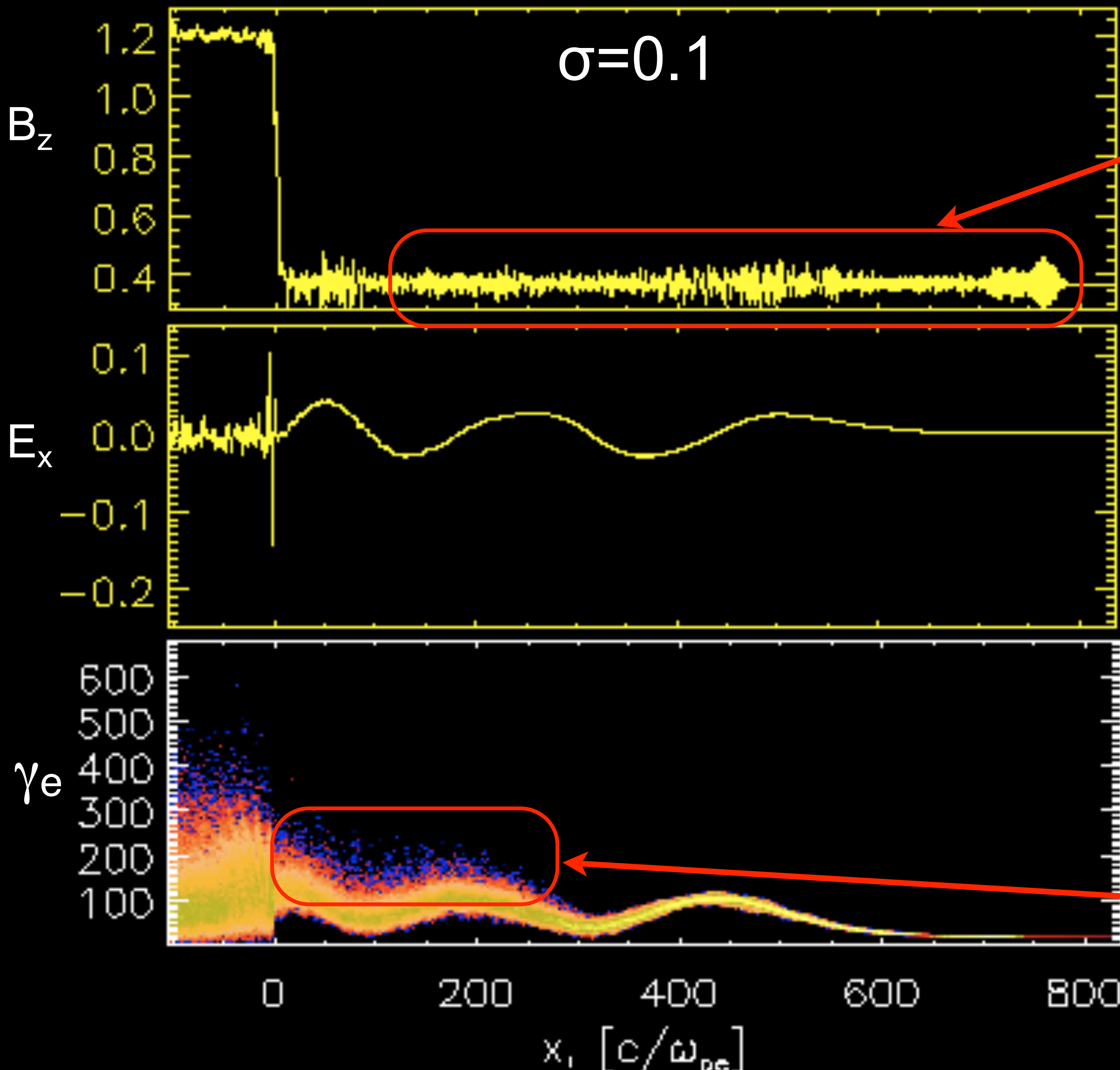

e.m. precursor wave
→ radiation pressure on electrons

electrostatic plasma oscillations

electron-ion energy exchange in upstream (Lyubarsky 2006)
→ electron heating & bulk acceleration before the shock (Iwamoto & Hoshino 19)

We expect lower efficiency (due to electron heating)

We expect lower frequencies (due to bulk acceleration)

Summary

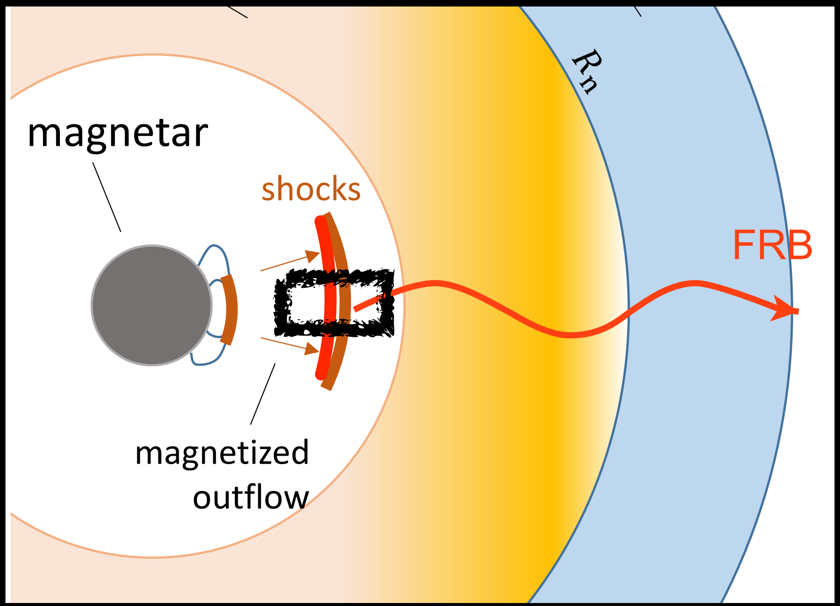

Beloborodov 17,19; Margalit & Metzger 18; Metzger, Margalit & LS 19; Margalit, Metzger & LS 20

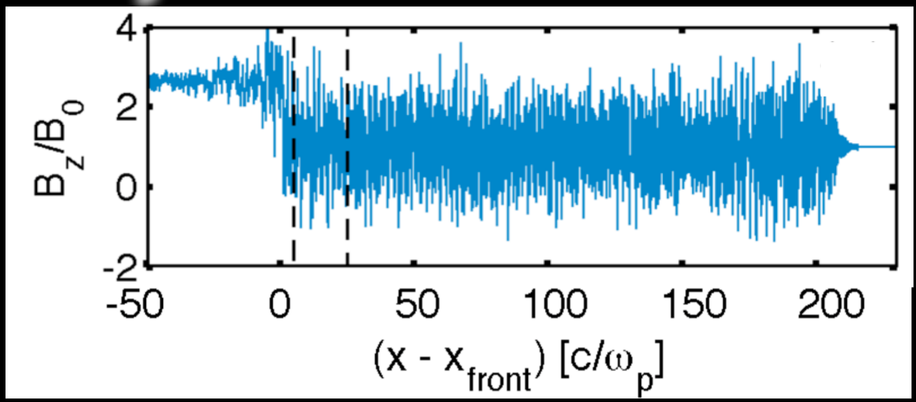

Building blocks of the model:

- magnetar flares drive relativistic magnetized shocks
- synchrotron maser at the shock produces the FRB
- shock decelerates

Implications of the model:

linear polarization for high σ

~ constant polarization angle

narrow-band ~GHz frequency bursts

downward frequency drift

possible fluence, duration, frequency correlations

high-energy (X,γ,optical) afterglow

(1) The wave strength

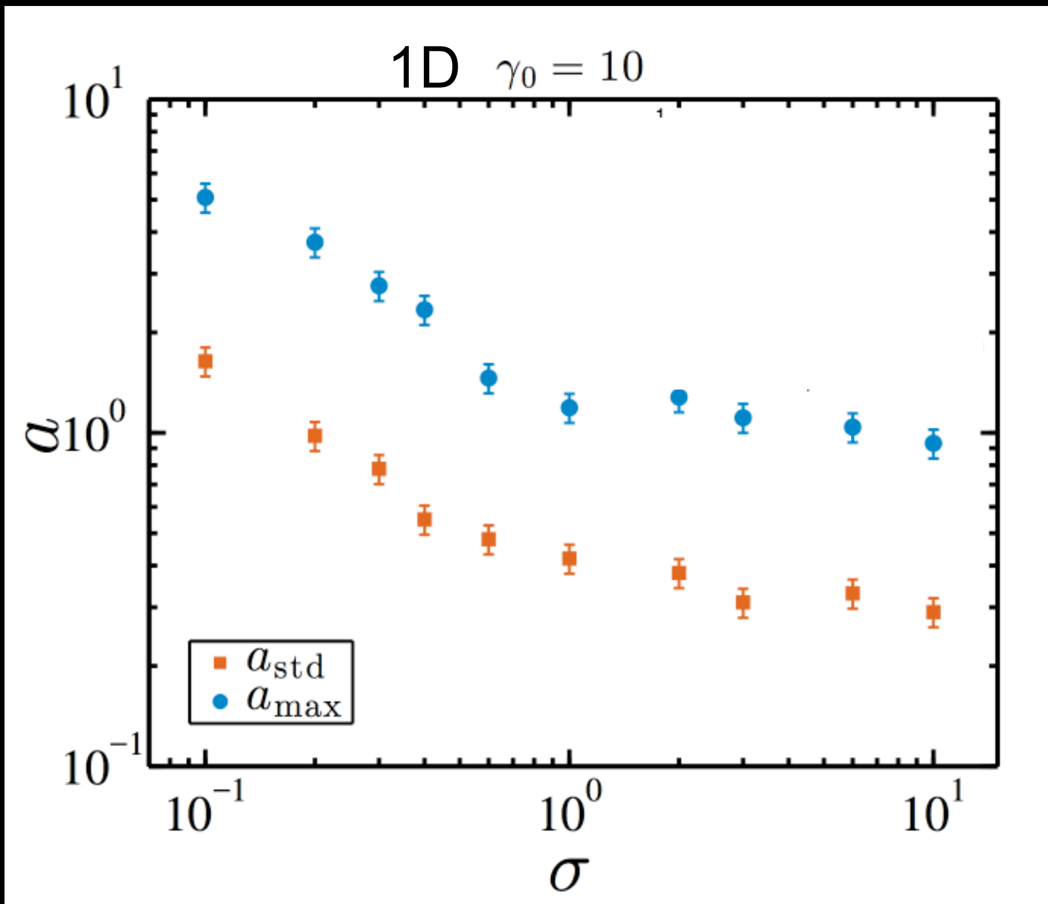

(Plotnikov & LS 19)

Wave strength / wiggler parameter:

$$a = \frac{e\,\delta E_y}{m_e c \omega}$$

Particles have transverse momentum oscillations ~ *a* m c

For FRBs, we expect *a*»1 (e.g., Margalit+20). What should happen?

- Relativistic bulk acceleration of upstream plasma away from the shock.
- Internal motions (heating) of upstream with typical momenta ~ *a* m c.

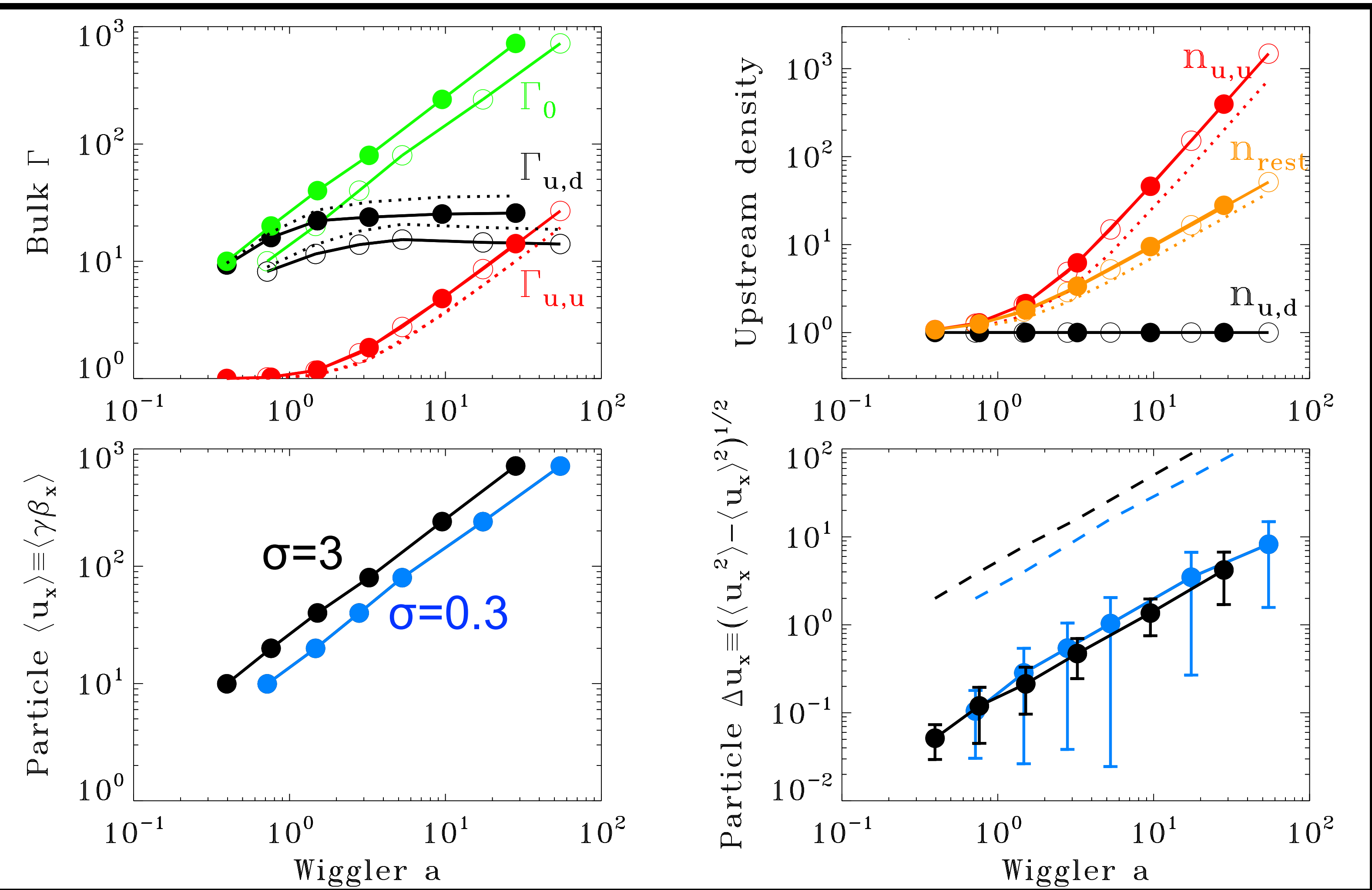

1D

- Bulk acceleration occurs, but the flux of particles into the shock stays the same.
- The mean energy per incoming particle is the same, and longitudinal heating is small.

(2) Spectrum

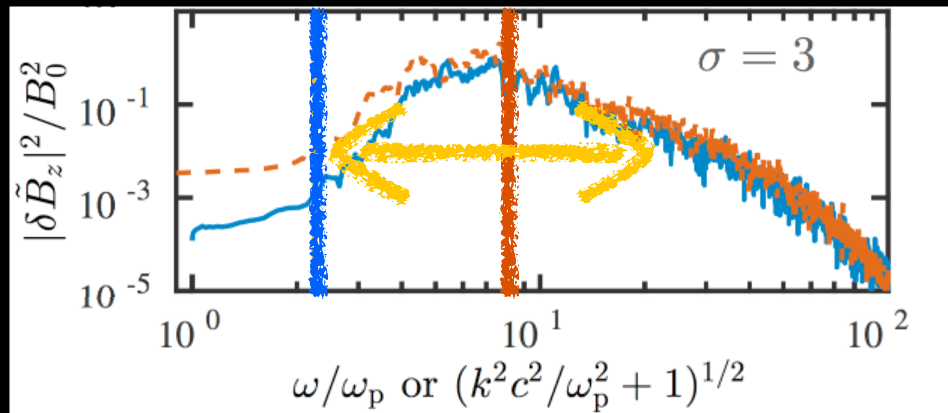

Low-frequency cutoff

Peak frequency

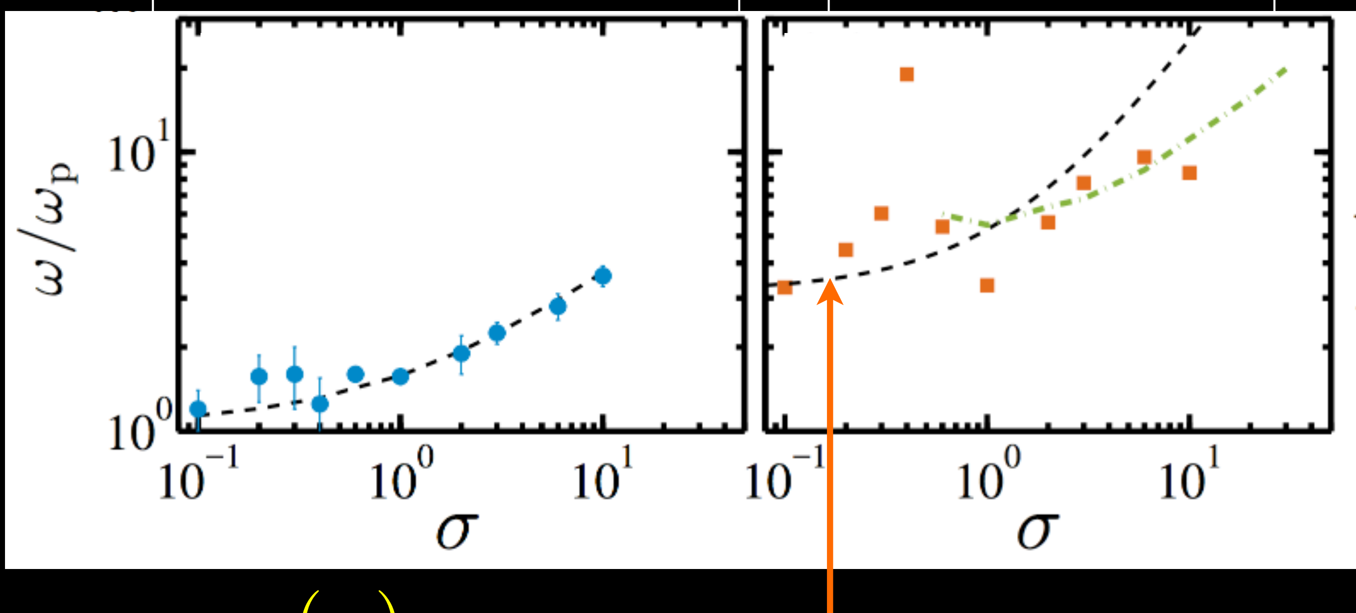

$$v_{ph}(\omega) = v_{sh}$$

cyclotron frequency in
shock-compressed field

Statistics of field fluctuations

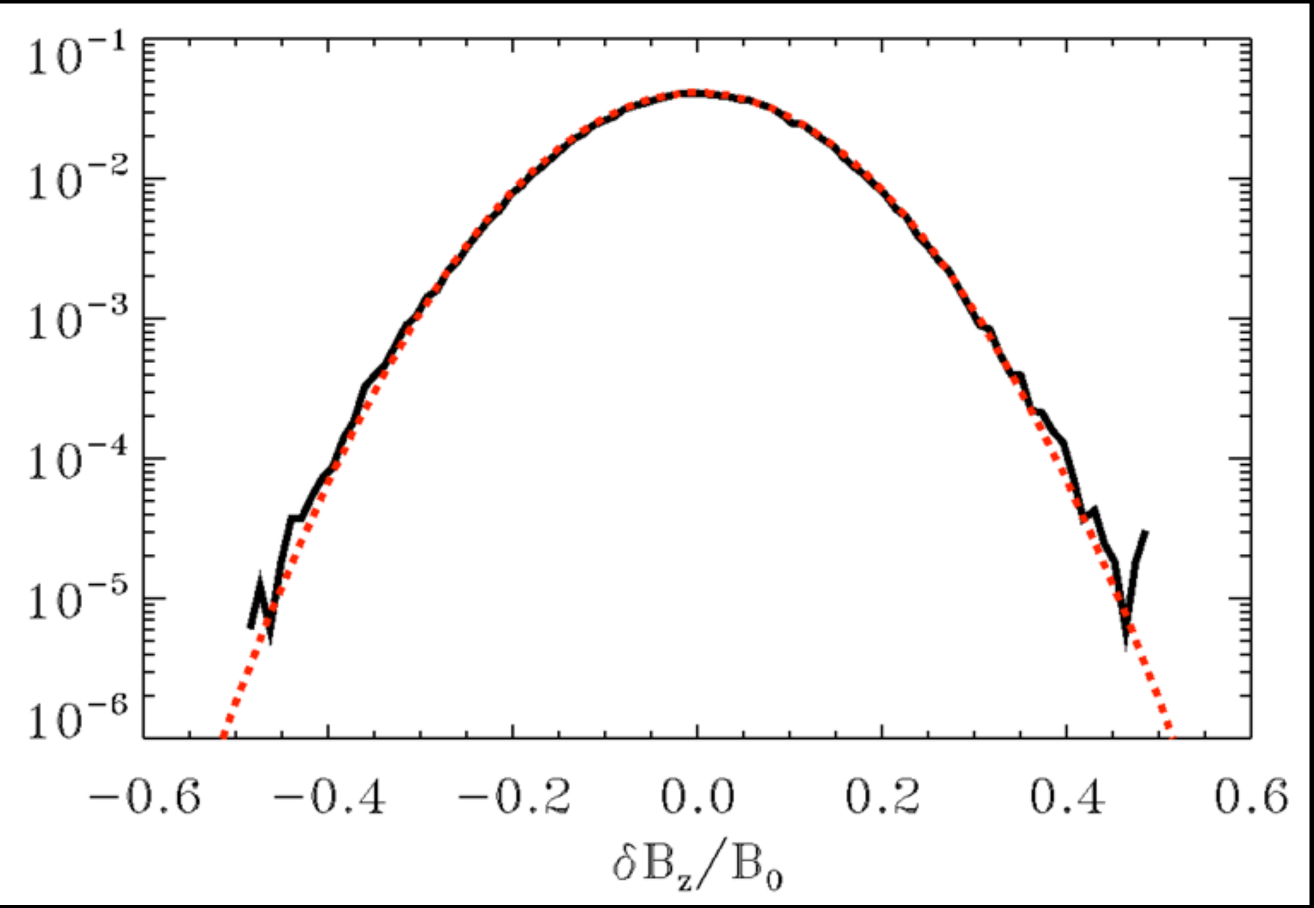

No departures from Gaussian.